8455
NACA TN 2028

TECH LIBRARY KAFB, NM
0065262

NATIONAL ADVISORY COMMITTEE FOR AERONAUTICS

TECHNICAL NOTE 2028

EFFECT OF TUNNEL CONFIGURATION AND TESTING TECHNIQUE ON CASCADE PERFORMANCE

By John R. Erwin and James C. Emery

Langley Aeronautical Laboratory
Langley Air Force Base, Va.

Washington
February 1950

AFMDC
TECHNICAL LIBRARY
AFL 2811

TECH LIBRARY KAFB, NM

0065262

NATIONAL ADVISORY COMMITTEE FOR AERONAUTICS

TECHNICAL NOTE 2028

EFFECT OF TUNNEL CONFIGURATION AND TESTING TECHNIQUE ON CASCADE PERFORMANCE

By John R. Erwin and James C. Emery

SUMMARY

An investigation has been conducted to determine the influence of aspect ratio, boundary-layer control by means of slots and porous surfaces, Reynolds number, and tunnel end-wall condition upon the performance of airfoils in cascades. A representative compressor-blade section (the NACA 65-(12)10) of aspect ratios of 1, 2, and 4 has been tested at low speeds in cascades with solid and with porous side walls. Two-dimensional flow was established in porous-wall cascades of each of the three aspect ratios tested; the flow was not two-dimensional in any of the solid-wall cascades.

Turbine-blade sections of aspect ratio 0.83 were tested in cascades with solid and porous side walls and blade sections of aspect ratio 3.33 were tested in cascades with solid walls. No particular advantage was observed in the use of porous walls for the turbine cascades tested.

INTRODUCTION

Airfoils are tested in cascades to provide fundamental information for the design of compressors and turbines. This information can be applied directly as basic data in many designs. The advantage of cascade testing lies in the relative ease and rapidity with which tests can be made, in the elimination of three-dimensional and boundary-layer effects not related to section performance, and in the much more detailed information concerning section performance which can be obtained in comparison with that obtainable from tests of rotating compressors and turbines. Cascade results have always contained inherent discrepancies, however, because the flow could not be made truly two-dimensional. These discrepancies arose from the interference and interaction of the boundary layers on the side walls with the flow about the test airfoils because of the finite aspect ratios necessarily used.

The data reported in references 1 and 2 are in some ways inconsistent and, in cross-plotting these data for design studies, irregularities appear such that the design would be indeterminate within the limits of required accuracy. These irregularities have caused much difficulty to persons attempting to interpolate or extrapolate the data for particular applications. Inconsistencies also arose from the fact that data from the Langley 5-inch cascade tunnel had always been subject to operating technique; for example, much skill and experience were necessary in adjusting the flexible floors correctly and data that were repeatable were difficult to obtain.

The specific difficulties that have led to distrust of previously obtained cascade data are:

(1) As was pointed out in reference 3, the lift coefficient obtained by integrating the pressure-distribution plots of reference 1 did not agree with that calculated from the measured turning angle, when two-dimensional flow was assumed.

(2) The fact that the pressure rise expected to result from the measured turning angle was not obtained obviously should have an effect on the magnitude of the turning angle; therefore some question arises as to the validity of the data in references 1 and 2. The pressure distribution is also affected in magnitude and in shape by the failure to obtain the calculated pressure rise.

(3) Compressor-blade sections of higher camber than could be satisfactorily tested in the original 5-inch cascade have been successfully used in a single-stage test blower (reference 4).

These effects are believed to be caused by the interaction of the tunnel-wall and test-blade-surface boundary layers since premature separation occurs at the juncture of the side walls and test blades and produces a large low-energy region at the exit from the cascade. This large wake acts as a restriction on the flow, higher average exit velocities result, and the flow is not two-dimensional.

Two-dimensional flow is believed to exist when the following criteria are satisfied:

(1) Equal pressures, velocities, and directions exist at different spanwise locations.

(2) The static-pressure rise across the cascade equals the value associated with the measured turning angle and wake.

(3) No regions of low-energy flow other than blade wakes exist. The blade wakes are constant in the spanwise direction.

(4) The measured force on the blades equals that associated with the measured momentum and pressure change across the cascade.

(5) The various performance values do not change with aspect ratio, number of blades, or other physical factors of the tunnel configuration.

Past attempts to establish two-dimensional flows in cascades have utilized boundary-layer removal slots on two or all of the tunnel walls upstream of the cascade, and cascades using blades of aspect ratio 4 or higher have been constructed. The present investigation was intended to determine the value of these methods and that of a method believed to be new, the use of continuous boundary-layer removal through porous surfaces from the cascade side and end walls. A representative compressor-blade section of aspect ratios of 1, 2, and 4 was tested at low speeds in cascades with solid and with porous side walls. This section was tested over a range of Reynolds number for each of these conditions. For comparison, turbine-blade sections in which the flow is characterized by a pressure drop through the test section were tested in cascades with solid and with porous side walls.

When schlieren or shadow photographs of flows through cascades are desired, the use of porous side walls would be difficult; therefore, several methods of correcting solid-wall-cascade results to the two-dimensional case have been compared and their accuracy discussed.

SYMBOLS

A	aspect ratio, span of blades divided by chord of blades
C_D	drag coefficient based on entering velocity, determined by wake survey
C_N	blade normal-force coefficient based on entering velocity
$(C_N)_P$	blade normal-force coefficient obtained by integration of blade pressure distribution
$(C_N)_M$	blade normal-force coefficient calculated from measured momentum and pressure changes
q	dynamic pressure, pounds per square foot
R	Reynolds number, based on blade chord and entering air velocity
V	velocity, feet per second

α angle of attack, angle between entering air and chord line of blade, degrees

β stagger angle, angle between entering air and a perpendicular to cascade stagger line, degrees

θ turning angle, angle through which air is turned by blades, degrees

σ solidity, chord of blade divided by gap between blades

Subscripts:

1 upstream of cascade

2 downstream of cascade

l local

c corrected

a axial

m mean value

t tangential

DESCRIPTION OF TEST EQUIPMENT

The test facilities used in this investigation were the Langley 5-inch and 20-inch cascade tunnels. The 5-inch cascade test section proper uses the same design and, to a considerable extent, the same parts as the one described in reference 1. A larger settling chamber having an area of about 25 square feet is used, however, and provides a ratio of settling-chamber area to test-section area of about 40:1. A similar settling chamber is used on the 20-inch cascade with an area ratio of only 10:1. It is believed that if a larger area ratio were used, this cascade would yield satisfactory entrance flows and less attention to the flexible-wall curvatures and suction pressure on the upstream slots would be needed. A sketch of a vertical cross section of either tunnel is shown as figure 1. Photographs of the two tunnels are presented as figures 2 and 3.

The porous surface is supported by a 120-mesh screen, which is in turn supported by a sheet of perforated metal having $\frac{1}{8}$-inch-diameter

holes with 1/4 inch between their centers in all directions. (See fig. 4.) This perforated sheet metal is available from steel suppliers as a standard item. A rigid frame of cellular construction is employed to carry the test airfoils and to minimize the bowing of the side walls due to the suction pressure. A number of different materials were investigated for use as porous surfaces; the results of this study are presented in a subsequent section.

The consideration that determined the particular cascade selected for detailed study was the desire to have as direct a comparison as possible with the present blading in the rotor of the 42-inch test compressor. The NACA 65-(12)10 compressor-blade section as used in this compressor has a stagger angle of 60° at the mean diameter and a solidity of 1.182 and is fairly typical of axial-flow compressor rotors. Because of the geometry of the cascade tunnel used, the sections were tested at a solidity of 1. This cascade has a relatively high static-pressure rise and high blade normal-force coefficient, conditions which make cascade testing difficult.

In addition, some data obtained at the less severe condition of 45° stagger are included to provide a more complete picture of the problem and of the results obtained.

The cascade of airfoils selected for detailed study was tested at low speed in the following tunnel configurations:

(1) 5-inch, blade aspect ratio 1, solid-wall cascade

(2) 5-inch, blade aspect ratio 1, porous-wall cascade

(3) 5-inch, blade aspect ratio 2, solid-wall cascade

(4) 5-inch, blade aspect ratio 2, porous-wall cascade

(5) 20-inch, blade aspect ratio 4, solid-wall cascade

(6) 20-inch, blade aspect ratio 4, porous-wall cascade

Turning-angle, pressure-rise, pressure-distribution, and wake-survey measurements were taken. For comparison purposes, results obtained by using a 42-inch-tip-diameter test compressor and a 28-inch-tip-diameter test blower are presented. All but wake-survey measurements were taken in the 42-inch test compressor described in reference 5. Turning-angle and pressure-rise measurements were obtained with the 28-inch test blower (reference 4).

The testing procedures used in this investigation were the same as those reported in reference 1. Most of the tests were made with a

fixed entrance velocity of about 95 feet per second and with blades of 5-inch chord. A few tests at other speeds were made to vary the Reynolds number. Tests on blades of aspect ratio 2 used airfoils of $2\frac{1}{2}$-inch chords. With the exception of tests run to determine proper end conditions, cascades of seven blades were used throughout.

In order to expedite plotting of test pressure-distribution results, a constant entrance dynamic pressure is normally used in cascade testing at the Langley Laboratory. Manometers scaled with values of q_l/q_1 are used so that no computing is required to make these plots. It is therefore convenient to obtain force coefficients on the basis of the entering dynamic pressures. All coefficients presented herein are so calculated.

The static-pressure rise across the test section can be controlled to a considerable extent by the quantity of flow drawn through the porous walls. The pressure rise corresponding to two-dimensional flow through the observed turning angle, when allowance for effective passage-area reduction due to the observed wake is made, could be established by this means. A chart of pressure rise or, more specifically, of q_2/q_1 was prepared for a range of turning angle and wake width for the test stagger angle and solidity (fig. 5). The effect of the blade wake on the exit velocity was taken into account by measuring the exit velocities and averaging the values for a few test points. A factor, dependent upon the wake width, was so obtained and was applied in computing values of q_2/q_1 for other conditions. This factor assumes that wakes of similar width will restrict the exit flow similarly. The validity of the curves was later confirmed by detailed velocity calculations for many tests. For all tests in which continuous boundary-layer removal was used, the pressure rise across the cascade was set by reference to the chart. Of course, this method was not applied to the series in which the pressure rise was intentionally made different from the two-dimensional value in order to examine the resulting effects.

RESULTS AND DISCUSSION

General

The investigations reported in references 1 and 2 used blades of aspect ratio 1. The results obtained, although providing useful information, failed to satisfy the criteria of two-dimensional flow. The Langley 20-inch cascade tunnel was constructed to permit blade models of aspect ratio 4 to be tested without reduction in blade chord

or test Reynolds number. The results for blades of aspect ratio 4 indicated that the static-pressure rise obtained did not agree with that calculated by using the measured values of turning angle and by assuming two-dimensional flow, even though correction was made for the blade wake measured at midspan. Further, the turning angles observed were quite different from the turning-angle values obtained in the test blowers. Correcting the data to account for the constriction due to separation near the walls failed to produce corrected turning angles in agreement with the values measured in the test blowers. When the data for the 5-inch blades of aspect ratio 1, which agreed with the data for the test blowers, were so corrected, however, the resultant values were lower than test-blower results. The values for the normal-force coefficient for the tests on blades of aspect ratio 4 appear to be in closer agreement with the values calculated on a basis of two-dimensional momentum and pressure changes when they are plotted with corrected turning angles than when the measured turning-angle values are used, but since the slopes of C_N against θ_c differ, the results are in question.

Thus it appears that cascades of aspect ratio 4 do not yield directly usable information even when axial-velocity corrections are applied. Because the blades are not operating under pressure-rise, turning-angle, and angle-of-attack conditions that represent the two-dimensional case, cascades of neither $A = 1$ nor $A = 4$ provide the conditions sought. Furthermore, large air supplies are required for high-aspect-ratio cascades, particularly for high-speed tests. For these reasons, attempts were made to devise methods that would provide two-dimensional flows in cascades using blades of low aspect ratio.

The interference and interaction of the tunnel-side-wall boundary layers with the boundary layers of the test airfoils were believed to be the reason for the flow not being two-dimensional. If the side-wall boundary layers could be removed continuously through the side walls, two-dimensional flow conditions could perhaps be established. In order to examine this possibility, the Langley 5-inch and 20-inch cascade tunnels were modified by replacing the test-section side walls with a frame supporting a perforated metal sheet and a porous material was attached to this perforated sheet. As illustrated in figure 2, a suction chamber connected to a blower was provided on the outside of the test section, and a part of the flow was drawn through the side wall. First tests using this system indicated considerable promise but also indicated that the material used for the porous surface affected the quantity of flow that had to be removed to establish two-dimensional conditions. For this reason, a search for suitable porous materials was initiated, and several were tested in the 5-inch cascade.

Other elements of the tunnel configuration that affect the character of the flow into the cascade are the entrance-cone shape, the

type, location, and number of the wall slots, and the treatment of the end wall. Only one modification of the circular-arc entrance-cone shape used on both tunnels was tried: The 20-inch-tunnel fairings were replaced with fairings of parabolic curvature in an attempt to eliminate the unfavorable pressure gradient that existed with the circular-arc cone. No measurable reduction of end-wall boundary-layer thickness was observed, however.

Test-Section Conditions for Two-Dimensional Flows

Porous materials.- Ideally, it would be desirable to employ permeable surfaces having varying porosity in order to distribute the boundary-layer removal in a manner related to the local boundary-layer thickness. No scheme that would be practical for a series of tests was evolved to accomplish this result. In a general way, a surface of uniform porosity accomplishes the desired result, for, where the pressure recovery has been the greatest, the quantity flowing through the surface will be greatest. The regions of highest pressure are unfortunately not necessarily regions where the boundary layer is thickest or most likely to separate, so a surface of uniform porosity is not ideal for compressor-cascade side walls. The surface porosity for these low-speed compressor-blade tests was determined by the requirement that the suction-chamber pressure be lower than the lowest pressure on the test airfoils. In this condition, the flow through the wall surface was everywhere outward from the test section to the suction chamber.

The first tunnel configuration using porous walls had a very heavy canvas as the surface. Because of the appreciable roughness of this material, a very large quantity of the main flow had to be removed through the canvas in order to obtain the pressure rise associated with the measured turning angle. Although a direct quantity measurement was not made, an estimate based on the suction pressure used would be that an air quantity of from 20 to 25 percent of the entering flow was removed through the walls. A medium-weight broadcloth material having a fairly smooth surface on one side was next tried. The quantity of air removed was 10.3 percent of the entering flow; this amount includes some leakage flow. Broadcloth surfaces were used for most of the tests reported herein.

One test using 2-ounce nylon sail cloth was run. This material appears to have desirable smoothness, strength, and abrasion-resistance properties, but the sample used was too closely woven for the conditions of the test. A flow volume sufficiently large to produce the required pressure rise through the cascade could not be removed with the existing suction blower. A very light parachute silk was also tried, but with the opposite result - the porosity was too great, and several layers

would have been required to obtain a satisfactory permeable surface. This arrangement was considered impractical for routine operations requiring many tunnel changes.

Several tests using a metal screen made by electroplating as the porous surface were run. The material, a copper-nickel alloy, has a very smooth, uniform surface, which is much smoother than wire screen of similar mesh (100), and is without the fuzz of cloth. The sample used had 16-percent open area. One or two layers of broadcloth backing were employed to produce the necessary resistance. A significant reduction in the porous-wall air removal was measured in the tests; the air removal dropped from the previous value of 10.3 to 4.5 percent of the main flow. Better agreement resulted between normal-force coefficients calculated from measured blade pressure distributions and those calculated by using the momentum equation. The electroplated metal screen was rather expensive, however. A porous surface formed by hammering copper or bronze screen was found to be very practical and quickly made. This technique is attributed to Mr. P. K. Pierpont of the Langley Full-Scale Research Division. By varying the number of hammering operations (each followed by torch annealing), a material of required porosity could be obtained. A screen successfully used over a wide range of test conditions had initial wire diameter of 0.014 inch, 30 mesh, and was hammered to a sheet thickness of 0.009 inch. The normal flow velocity plotted against pressure drop for this material is presented in figure 6.

No comparative tests were run in the 20-inch tunnel, but it is believed that a similar reduction in porous-wall air removal could have been achieved; however, a typical value for this removal in the 20-inch tunnel is 2.9 percent when broadcloth is used. This percentage was so small that attempts to reduce the amount seemed unnecessary.

Slot configurations.- A series of runs was made with several combinations of tunnel side- and end-wall slots in order to produce uniform entering flows and to reduce porous-wall suction flow quantity. The possibility of using flush side-wall slots was considered, since flush side slots would eliminate the width change in the end plates and would increase the ease and decrease the time of operation. The tests were made by using existing sharp-edge protruding slots with and without fairings in order to vary the configuration and so do not represent optimum slot shapes. The side-wall slots were closed by fairings extending from the entrance cone to the slot; these fairings reduced the tunnel width to a constant 5 inches. An increase of 2 percent of the main flow or 21 percent of the permeable-wall flow was required to establish the desired cascade pressure rise.

The fairing was then moved 1/8 inch upstream to produce a flush slot, and 10.5 percent of the main flow was drawn through the porous wall

when 8.8 percent was removed through the flush slot. An increase in slot suction pressure, which raised the slot flow to 11.4 percent, decreased the required porous-wall flow only slightly to 10.3 percent of the main flow. Increasing the flush-slot width to 1/4 inch had a detrimental effect on the required flow through the cloth wall. A different slot shape similar to that recommended in reference 6 might have improved the performance, but this possibility has not yet been investigated. Flush slots parallel to the cascade stagger line might be expected to deflect the entering flow at stagger angles other than zero. In these tests, however, this effect was not measurable when the static-pressure drop through the slot was less than one-half the dynamic pressure entering the cascade. For the usual range of cascade stagger angles, no greater static-pressure drop than one-half the entering dynamic pressure has been found necessary.

The few tests run to determine the end-wall slot configuration indicated the same trends as the side slots. The protruding slots were slightly more effective than flush slots, but only an insignificant reduction in air removal was gained over the sealed or no-slot condition. However, when seven blades were used with the end blades serving as the cascade boundary, boundary-layer removal was necessary. Without the end slots, separated turbulent flow occurred over the end blades, and apparently uniform entering conditions for the cascade could not be established.

Figure 7 shows the boundary-layer profile measured at several stations about 1 chord upstream of the cascade. The origin of each of the small plots is placed at the survey point. It is evident that the protruding slot produces a clean flow at these locations.

End conditions.- In order to study the effect of the end gap on the behavior of the main flow, a few tests using five blades were run with varying end gaps. A blade equipped with orifices was placed nearest the end walls. As indicated in figure 8, in the case of the half-gap end spacing, the last blade did not carry lift equal to that of the central blade. When the end spacing was increased to a whole gap, the lift on the end blade increased considerably, although not up to the value of lift on the central airfoil. The important result, however, is that the change of end gap had no measurable effect on the performance of the central blade. The pressure distribution, turning angle, and drag coefficient remained as before.

Other investigators have used the end blades in the cascade as the boundary (reference 7). In order to examine the possibilities of this method, two extra blades were installed in the 5-inch cascade tunnel. Runs were first made with the end walls sealed to the end blades at their approximate stagnation points. This system provided too few variables, and proper entering conditions could not be established;

in addition, the end passages exhibited stalling and fluctuating flows. The end walls were moved outward about 1/2 inch for the subsequent test, and a gap between the flexible end walls and the end blades resulted. Attempts to control the entering static pressure and direction of flow by bending the end walls were made. Considerable stalling continued to occur, however, apparently because of the thick end-wall boundary layer. To investigate this possibility a $\frac{3}{16}$-inch protruding slot was built into the upper and lower end walls 1 chord ahead of the test blades. These slots were ducted to an exhauster. Satisfactory control of entering conditions was possible by bending the flexible surfaces. Some operating time is eliminated with this system since it is not necessary to set the end wall exactly in the direction of the exit flow, and less skill and time are required in adjusting the entering conditions. However, the flow about the central blade appeared to be the same as that for the other two satisfactory tunnel configurations.

The number of blades required in a cascade appears to be an inverse function of the amount of time and care employed in establishing the end conditions. With the flexible end walls used in the cascades described herein, little difference in performance was noticed between similar configurations of five or seven blades. In a setup where end-wall adjustments are not readily made or where running time is limited to a few minutes, significant differences in the performance might be observed.

In tests of airfoils more highly cambered than the NACA 65-(12)10 section reported herein, continuous boundary-layer removal on the convex end wall has been necessary in order to prevent separation from this wall and to permit uniform exit flow from the cascade. A porous surface beginning at the end-wall slot, about 1 chord upstream of the blades, was extended through the cascade to about 1 chord downstream of the blades. Provision was made for flexing this end wall to the desired curvatures. Although continuous boundary-layer removal might also be desirable for the concave end wall, the additional complexity is undesirable. A thin sheet-brass end wall has been found to provide satisfactory flows at a stagger angle of 60° and at a turning angle of 30°, which is a rather severe case.

Comparison of Cascade and Test-Blower Results

Turning angle and static-pressure rise.- Results for the several cascades and test blowers investigated are given in figures 9 and 10 as plots of turning angle against angle of attack. All test airfoils are the NACA 65-(12)10 section. All stagger angles are 60° and all solidities are unity, with the single exception of the 42-inch-diameter test compressor, in which a mean diameter solidity of 1.182 existed,

and in which the stagger increased with angle of attack so that $\beta = 60^{\circ}$ occurred at $\alpha = 14^{\circ}$. Turning-angle corrections obtained from reference 2 for varying stagger angle in the 42-inch compressor are presented. Because the rotor-blade solidity was 1.182, the turning angles measured in the 42-inch compressor were predicted to be about 0.4° higher than in the 28-inch test blower or cascades of solidity 1.

If the results of the solid-wall cascade tests are compared, an increasing turning angle with increasing aspect ratio is very evident. The results from porous cascades and test blowers agree with the data from the solid-wall cascade of aspect ratio 1. This behavior is believed to be due to counteracting effects. The velocities induced by the trailing vortices due to reduced lift in the tunnel-wall boundary layers and the movement of the wall boundary layer onto the suction surface of the airfoils have an over-all result of reducing the blade lift and hence the net turning angle. A factor having an opposite effect is the increase of axial velocity resulting from thickened wall boundary layers (see reference 3). That this effect exists is evident during operation of the porous-wall cascades: As the porous-wall flow is increased and the pressure rise across the cascade is increased, a measurable reduction in turning angle takes place. Figure 11 shows this effect for the cascade with blades of aspect ratio 4.

In a recent paper (reference 8), Hausmann has presented an analysis of the simplified trailing-vortex problem. In the rather severe case calculated, the indication is that the turning angle would be increased because of the downwash associated with the trailing vortices. The opposite effect is predicted by Carter and Cohen in reference 9. A discussion of these counteracting effects is presented in a subsequent section, with the conclusion that no method is now available to explain satisfactorily the flows observed in the solid-wall cascades.

The solid-wall cascades studied failed to produce the pressure rise associated with the measured turning angles (fig. 12). At low aspect ratio the three-dimensional effects predominated, and low turning angles were observed. With higher aspect ratios, the induced effects were of smaller magnitude, and more turning of the flow resulted. To approach two-dimensional flows in solid-wall cascades, aspect ratios much greater than 4 must be used.

Satisfactory agreement of θ with α and q_2/q_1 with θ was obtained between porous-wall cascades of aspect ratios of 1, 2, and 4 and two test blowers at their mean diameters. The porous-wall cascades appear to satisfy these criteria of two-dimensionality.

Passage wake surveys.- An examination of the flow downstream of the cascade was made in order to determine how much of the flow was homogeneous. Total-pressure surveys of the test cascade were made in the solid- and porous-wall configurations with blades of aspect ratio 1 at an angle of attack of 15.1°. The results are presented in figure 13. In the solid-wall case, a large region of low-energy air, which had its core originating at the junction between the convex surfaces of the test airfoil and the tunnel wall, was observed. In reference 9, a similar plot is presented for a cascade of aspect ratio 2 in which similar results are indicated. The percentage of the flow area affected is less, however, and a short region of uniform flow appears in the center of the tunnel.

The porous-wall configuration had only a relatively small region of loss greater than that of the wake of the test blades. The portion of the wake unaffected by the spread near the wall was 80 percent of the tunnel width. The total-pressure-loss values in this "two-dimensional" wake were lower and of smaller extent than in the solid-wall test.

A comparison of these plots illustrates clearly how continuous removal of the wall boundary layers alters the static-pressure rise across a compressor cascade. With solid walls, the large low-energy regions act to constrict the main flow and so reduce the effective flow area, so that an increase in the main exit flow velocity results. With permeable walls, since the effective exit flow area is much larger, the exit velocity is smaller and the static-pressure rise is higher.

Comparison of normal-force coefficients.- One of the important criteria for two-dimensional flow is that the value for the force on the blades determined by calculation of the momentum and pressure changes associated with the measured turning angle be equal to the force as determined by integration of the surface pressures. The ability of the configurations used to satisfy this criterion is illustrated in figure 14. The solid-wall cascade of aspect ratio 1 fails badly. The solid-wall cascade of aspect ratio 4 is better but the normal-force coefficient obtained from pressure distributions is from 7 to 15 percent low. The porous-wall cascades are clearly superior on this count, because reasonable correlation between $(C_N)_P$ and $(C_N)_M$ is indicated over the usual operating range.

Figure 15 shows that good agreement was obtained between $(C_N)_P$ and $(C_N)_M$ with the porous-wall cascade of aspect ratio 1 at the lower-pressure-rise case of $\beta = 45^\circ$. No tests at lower than 45° stagger were included in this investigation, but it is believed that satisfaction of all the criteria of two-dimensionality would be obtained.

The pressure rise across the cascade has an effect on the force normal to the blade. In order to calculate this force, the pressure rise must be known or assumed. The calculated normal-force-coefficient curves of figures 14 and 15 were prepared by using the pressure rise measured in the porous-wall cascades. As previously noted, the values of q_2/q_1 are controllable with continuous boundary-layer removal and were adjusted to correspond to the observed turning angle with allowance for the observed wake. The calculated values of C_N presented are therefore believed to be representative of two-dimensional flow and the most logical basis for comparison.

An interesting comparison is that of the pressure-distribution normal-force coefficients obtained with the 1000-horsepower blower, the values calculated for the observed turning angles and the values obtained in solid-wall cascade of aspect ratio 1. This cascade might be expected to produce effects similar to the blower, if the physical similarity were the determining factor, since the 1000-horsepower blower has blades of aspect ratio of about 1, solid "walls," and a solidity of 1.182. The values of σC_N presented in figure 16 illustrate that the effects are not similar. At the mean diameter, the test-blower σC_N values match the values calculated for the measured turning angles within the limits of the measuring accuracy, but the values for the solid-wall cascade of aspect ratio 1 are greatly different.

The excellent agreement between the test blowers and the porous-wall cascades on turning-angle (θ against α), normal-force-coefficient ($(C_N)_P$ and $(C_N)_M$ against θ), and pressure-rise (q_2/q_1 against θ) relations probably results from the relatively greater energy of the boundary layers in the blowers compared with the energy of the boundary layer in the cascade tunnels. This energy difference, which is due to greater relative velocities between the boundary layer and the running blades in the blowers as compared with the stationary blades in the cascade, is discussed in reference 3. The excellent agreement obtained illustrates that two-dimensional cascade data can be used directly in the design of axial-flow compressors.

Spanwise pressures.- One of the characteristics of a flow constant in the spanwise direction is that equal pressures exist at one chordwise position at different spanwise locations. In order to examine the ability of the various setups to meet this requirement, airfoils having static-pressure orifices located 1/2 inch from the tunnel wall as well as at the usual center-line location were constructed. NACA 65-(12)10 compressor blades of aspect ratio 1 were tested at 60° stagger, with a solidity of 1, with solid and with porous walls. In the solid-wall case (fig. 17) the pressures near the wall are quite different from those along the tunnel center at the various chordwise stations. In addition, the normal-force coefficient obtained by integrating the

center-line diagram is significantly lower than that calculated from the measured turning angle. This fact, coupled with the difference between the measured and calculated exit velocities, suggests that significant differences in the pressure distribution would occur either in the ideal two-dimensional case or in a compressor (the calculated pressure rise has been obtained in several test blowers). This possibility was discussed in reference 3.

Pressure distributions similar to those for the solid-wall condition are presented in figure 18 for the porous-wall condition. Excellent agreement is obtained between the two diagrams. The normal-force coefficients obtained by integration and by calculation agree within the limits of experimental error.

For purposes of comparison, the center-line pressure distributions of figures 17 and 18 have been replotted in figure 19. Although the angle of attack and turning angle were similar in the solid-wall test, it is clear that the total area is considerably less and that the pressure distributions differ from each other in such a manner that it would be difficult, if not impossible, to devise a method for correcting the solid-wall test results to agree with those which would result in a two-dimensional flow.

Similar agreement was obtained in porous-wall tests at a stagger angle of 60° with a cascade of aspect ratio 4 (fig. 20) over the test range of angle of attack. It is therefore believed that a reasonably close approach to two-dimensional flow was obtained with continuous removal of the tunnel-wall boundary layers.

Effect of Reynolds Number

A set of 2.5-inch-chord airfoils was constructed to permit cascade tests with blades of aspect ratio 2. At the usual test velocity of about 95 feet per second, the Reynolds number of this cascade would be 123,000, a value presumably well above the critical range at which scale effects occur (usually taken to be about 100,000 for typical axial-flow compressors). Because of the low turbulence level of the Langley 5-inch cascade tunnel, laminar separation existed, and very poor performance was observed. (Velocity variation was 0.0004 of stream velocity; however, in both tunnels the turbulence factor varied somewhat with the air velocity.) A series of tests was therefore run in an attempt to define the critical Reynolds number for the test cascade in several tunnel configurations.

The 2.5-inch-chord blades in the original smooth condition were tested at several values of R by increasing the test entrance velocity. In figure 21, a leveling of the turning-angle and drag-coefficient

curves around values of $R = 250,000$ is indicated for these tests. Because the tunnel motor and blower appeared to be operating at speeds above a safe limit, attempts to simulate higher effective values of R by introducing turbulence into the air stream and by using airfoils roughened by a strip of masking tape at the leading edge were made. Figure 22 indicates that a turning-angle performance indicative of higher effective Reynolds number can be obtained by the use of roughness. Some difficulty was encountered in introducing turbulence to the test air stream and still maintaining uniform entering-flow conditions, so the results are not presented herein. However, qualitatively, the expected effect was observed.

To make certain that values of R above 250,000 would produce only insignificant changes in performance, a set of 5-inch-chord airfoils were rerun in the 5-inch cascade with solid walls at the usual test velocities and at higher values. These results are included in figure 21. Since the aspect ratio of the blades used in these tests was unity, the turning-angle values are not directly comparable with the results of the 2.5-inch-chord tests. The indication is that the critical Reynolds number is about 250,000.

Hot-wire anemometer measurements in the 20-inch tunnel indicated that the turbulence factor of this tunnel was about ten times that of the 5-inch tunnel. To obtain further information on Reynolds number effects, the test cascade was rerun in the 20-inch tunnel. Entering speeds above and below the usual value were used. These results are also included in figure 21. In the Reynolds number range between 160,000 and 250,000 the turning-angle values for the porous-wall cascades of $A = 1$ and $A = 4$ vary less with R than do the values for solid-wall cascades of $A = 2$. Apparently, continuous removal of the side-wall boundary layer makes a compressor cascade less sensitive to Reynolds number changes.

A large variation in the value of the measured drag coefficient is noted at $R = 250,000$. The section drag for the solid-wall cascade of $A = 1$ is influenced by the blade-wall junction losses, as was shown in figure 13. The drag coefficient of the test airfoils of $A = 2$ in the solid-wall cascade and $A = 1$ in the porous-wall cascade is believed to be greater than that of the airfoils with $A = 4$ because of the greater turbulence and higher effective Reynolds number in the 20-inch tunnel. This trend is evident in figure 23, in which a plot of C_D against α is presented for several tunnel configurations. The scatter of the drag values suggests the order of accuracy of this measurement.

Data taken at angles of attack other than 15.1° indicate a large change in the values of $d\theta/d\alpha$ with R (fig. 24). Most of these data

were obtained with the solid-wall cascade with blades of $A = 2$, over only a 4° range of α; however, a more complete α range was run in a porous-wall cascade with blades of $A = 2$ at $R = 190,000$ and 176,000. The points presented in figure 24 are not to be considered final, but they do provide an indication of the trend to be expected.

The decrease of $d\theta/d\alpha$ with R is believed to be related to the pressure gradients near the leading edge of the convex surface of the test airfoils and to the extent of the laminar separation. At lower angles of attack, the pressure recovery in the forward 35 to 40 percent chord is small (fig. 20) and laminar flow can exist for some distance so that a relatively thick laminar boundary layer results. Farther downstream a rapid pressure rise occurs and, at low Reynolds numbers, a severe laminar separation takes place and low lift and low turning angles result. The fact that severe separation occurs is indicated by the high drag values measured at low Reynolds numbers (fig. 21). At higher angles of attack, the region favorable to a laminar boundary layer is reduced, so that when laminar separation takes place the separation is of lesser extent. (In some cases, particularly at higher Reynolds numbers, the flow may reattach to the surface.) Thus, as the angle of attack is increased, a disproportionate increase in turning angle occurs at low Reynolds numbers. At higher Reynolds numbers, laminar separation is less likely to occur so these effects are less pronounced and a lower value of $d\theta/d\alpha$ results.

Attempts were made to verify the apparently reduced effect of Reynolds number on porous-wall cascades of aspect ratio 1 and 4 by testing the 2.5-inch-chord airfoils of $A = 2$ with permeable walls. With the exhausting equipment available, it was not possible to establish the desired flow conditions at Reynolds numbers above 190,000. At this value, a turning angle of 19.2° was measured at 15.1° angle of attack, and $d\theta/d\alpha$ equalled 0.90. These results agree with the previously recorded data.

Comparison of Several Methods of Correcting Turning Angles to the Two-Dimensional Case

There are many situations in which it would be desirable to use solid-wall cascades if suitable means for correcting the results were available, as, for example, when schlieren photographs of the flow are desired. Several methods for converting cascade and blower results that are not two-dimensional to the two-dimensional case were applied to the data from the solid-wall cascade with blades of $A = 4$. One method is based on the discussion in reference 3, in which the exit axial velocity is made equal to the inlet axial velocity. The entrance stagger angle and angle of attack are assumed to be unaffected by the exit flow

(fig. 25(a)). A second method, based on a discussion in reference 10, suggests that the exit axial velocity be adjusted by one-half the difference between inlet and exit values, and the corrected turning angle be the difference between the actual inlet vector and the adjusted exit vector (fig. 25(b)). A third method is to average the inlet and exit axial velocities and then reduce the averaged axial velocity by one-half the axial-velocity increment due to the wake to obtain the inlet axial velocity. The exit axial velocity would be greater than the average value by one-half the wake increment (fig. 25(c)). In all these methods, the change in the tangential velocity is assumed to be unaffected by the change in axial velocity. This assumption may not be valid.

The turning angles measured in the solid-wall cascade of $A = 4$ have been corrected by these three methods, and the results are presented in figure 26. The turning angles measured in the solid-wall cascade of $A = 1$, which were in good agreement with test-blower and porous-wall-cascade results as indicated in figure 9, are included in figure 26. Corrected values obtained by the wake-allowance method (method III), which gave the smallest change for a given axial-velocity increase, are also included for the $A = 1$ solid-wall case. The turning angles for the $A = 4$ case as measured were 2° to 4° higher than the median values of figure 10. The second and third methods reduced these differences to about one-half. The first method yielded results in better agreement with the median curve, but the corrected values tended to be low, with a maximum difference of about 1°.

The wake-allowance method was applied to the data from the solid-wall cascade with blades of $A = 1$. The corrected turning angles appear 2° to 3° below the measured data (or the median curve) if this method is used and would be even lower if the other methods were used. Since the corrected turning angles for blades of $A = 4$ tend to be too high and the values for blades of $A = 1$ too low, the conclusion might be drawn that some combination of test aspect ratio and correction method could be obtained that would make possible the adjustment of cascade data that are not two-dimensional to the two-dimensional case. That such a combination would yield satisfactory results over the useful range of stagger angles, solidities, and cambers seems unlikely. Consideration of correction attempts for aspect ratios 1 and 4 indicates that a single simple method of adjusting measured values for observed axial-velocity changes is not likely to be found. Apparently factors other than the increase or decrease of axial velocity through the cascade must be taken into account. Undoubtedly one of these other factors is the effect of the flow induced by the trailing vortices. The method of reference 9 was used to estimate the magnitude of these effects in the solid-wall cascades of $A = 1$ and $A = 4$, for a measured turning angle of 20°. The turning angle in the cascade of $A = 1$ is decreased about 2° by the induced flow, while the turning angle for the blade of $A = 4$ is reduced by 1.7°. Adding 2° to the corrected turning

angles in figure 26 would bring the $A = 1$ results into closer agreement with the median curve. Adding 1.7° to the $A = 4$ results, however, would cause greater disagreement between the values corrected by any of the three methods used and the median curve of figure 10.

The values of normal-force coefficient obtained by integrating the pressure distribution about the test airfoils have been replotted with the turning angles corrected by three methods (fig. 27). The corrected $(C_N)_P$ curves intersect the theoretical curve within the test range. The $(C_N)_P$ curve plotted against measured values of θ did not intersect the theoretical curve (fig. 14). Thus the axial-velocity adjustment methods used might be considered to improve the agreement between measured and calculated normal-force coefficients, but, because the slopes are quite different, only little improvement is gained. If the induced flows were taken into account by the relations of reference 9, the various values of $dC_N/d\theta_c$ would be in less agreement with the theoretical values, because the reduction of turning angle due to the trailing vortices increases with C_N. Thus no methods are at hand to explain the observed flows in the solid-wall cascades.

Turbine-Blade Tests

A turbine blade designed to operate at $\beta = 30^{\circ}$ with about 85° turning angle, a pressure-drop, reaction condition, was tested in the 5-inch tunnel in cascades of $A = 0.83$ and in the 20-inch tunnel in cascades of $A = 3.33$; solid walls were used. The curves of α against θ are presented in figure 28. Little difference other than experimental scatter is noted. Blade-surface static-pressure measurements taken along the tunnel center line are shown in figure 29. Greater differences than can be accounted for by inaccuracies of measurement existed, but general agreement was obtained. Tuft surveys indicated a collecting of low-energy flow at the juncture of the convex surface of the test blades and the tunnel side walls. In these tests, even at the lower aspect ratio, this condition seemed to have little effect on the test results. It is therefore believed that, with usual pressure-drop cascades, as with reaction turbine blades, nozzles, and guide vanes, useful results can be obtained with cascades of low aspect ratio.

Another reaction turbine section designed for 105° turning at 45° stagger was tested in the 5-inch tunnel in cascades of $A = 0.83$ with solid and with porous walls. Since the dynamic pressure at the exit from the solid-wall cascade was not much greater than that calculated for two-dimensional flow, very little air could be drawn through porous walls without lowering the exit dynamic pressure below the desired value. With this low porous-wall flow rate, the pressure drop across the porous walls in use with this test was not sufficiently

great to produce an inflow through the entire wall. Therefore, the flow through the cascade could not be considered valid. Nevertheless, a turning angle only 1° different (in 105°) was measured. This test is at best only indicative of the effects of using porous walls with turbine cascades, but it seems clear that with pressure-drop cascades little benefit is to be gained through the use of permeable side walls.

CONCLUSIONS

The results of an investigation to determine the influence of aspect ratio, boundary-layer control by means of slots and porous surfaces, Reynolds number, and tunnel end-wall condition upon the performance of airfoils in cascades have led to the following conclusions:

1. Conventional cascades of compressor blades with aspect ratio 4 do not simulate the two-dimensional case. The indication is that very large aspect ratios would be necessary to satisfy all criteria of two-dimensionality.

2. Because of opposing effects, the solid-wall cascade of aspect ratio 1 produced a relation between turning angle and angle of attack for the NACA 65-(12)10 compressor blade at a solidity of 1 and a stagger of 60° more nearly like that of two test blowers than that of the solid-wall cascade of aspect ratio 4. However, the normal-force coefficients obtained from the measured pressure distributions were significantly less than those calculated from momentum and pressure changes, and the measured pressure rise across the cascade was significantly less than that associated with the measured turning angle.

3. With continuous boundary-layer removal, cascades of aspect ratios 1 and 4 produced curves of turning angle against angle of attack for the NACA 65-(12)10 airfoil very similar to those of two test blowers, when the pressure rise associated with the measured turning angle was established.

4. Much better agreement was achieved with the porous-wall cascades between the normal-force coefficients calculated from momentum and pressure changes and those obtained by integration of the measured pressure distributions than was obtained with the solid-wall cascades.

5. With cascades having a decrease in static pressure in the downstream direction, as with guide vanes and turbine blades, the use of permeable walls appears to be of negligible advantage. With such cascades, tunnel configurations having blades of aspect ratios of 0.83 and 3.33 produced similar results.

6. For typical compressor-blade cascades in tunnels of low turbulence level, scale effects seem to be negligible above Reynolds numbers of 250,000 but may be appreciable below this value.

7. The porous-wall technique as applied to cascades of compressor blades makes possible the attainment of two-dimensional flows.

Langley Aeronautical Laboratory
National Advisory Committee for Aeronautics
Langley Air Force Base, Va., November 30, 1949

REFERENCES

1. Bogdonoff, Seymour M., and Bogdonoff, Harriet E.: Blade Design Data for Axial-Flow Fans and Compressors. NACA ACR L5F07a, 1945.

2. Bogdonoff, Seymour M., and Hess, Eugene E.: Axial-Flow Fan and Compressor Blade Design Data at 52.5° Stagger and Further Verification of Cascade Data by Rotor Tests. NACA TN 1271, 1947.

3. Katzoff, S., Bogdonoff, Harriet E., and Boyet, Howard: Comparisons of Theoretical and Experimental Lift and Pressure Distributions on Airfoils in Cascade. NACA TN 1376, 1947.

4. Herrig, L. Joseph, and Bogdonoff, Seymour M.: Performance of an Axial-Flow Compressor Rotor Designed for a Pitch-Section Lift Coefficient of 1.20. NACA TN 1388, 1947.

5. Runckel, Jack F., and Davey, Richard S.: Pressure-Distribution Measurements on the Rotating Blades of a Single-Stage Axial-Flow Compressor. NACA TN 1189, 1947.

6. Pierpont, P. Kenneth: Investigation of Suction-Slot Shapes for Controlling a Turbulent Boundary Layer. NACA TN 1292, 1947.

7. Howell, A. R.: Fluid Dynamics of Axial Compressors. Proc. Inst. Mech. Eng. (London), vol. 153, 1945, pp. 441-452. Reprinted in U. S. by A.S.M.E.

8. Hausmann, George F.: The Theoretical Induced Deflection Angle in Cascades Having Wall Boundary Layers. Jour. Aero. Sci., vol. 15, no. 11, Nov. 1948, pp. 686-690.

9. Carter, A. D. S., and Cohen, Elizabeth M.: Preliminary Investigation into the Three-Dimensional Flow through a Cascade of Aerofoils. R. & M. No. 2339, British A.R.C., 1946.

10. Hawthorne, W. R.: Induced Deflection Angle in Cascades. Jour. Aero. Sci. (Readers' Forum), vol. 16, no. 4, April 1949, p. 252.

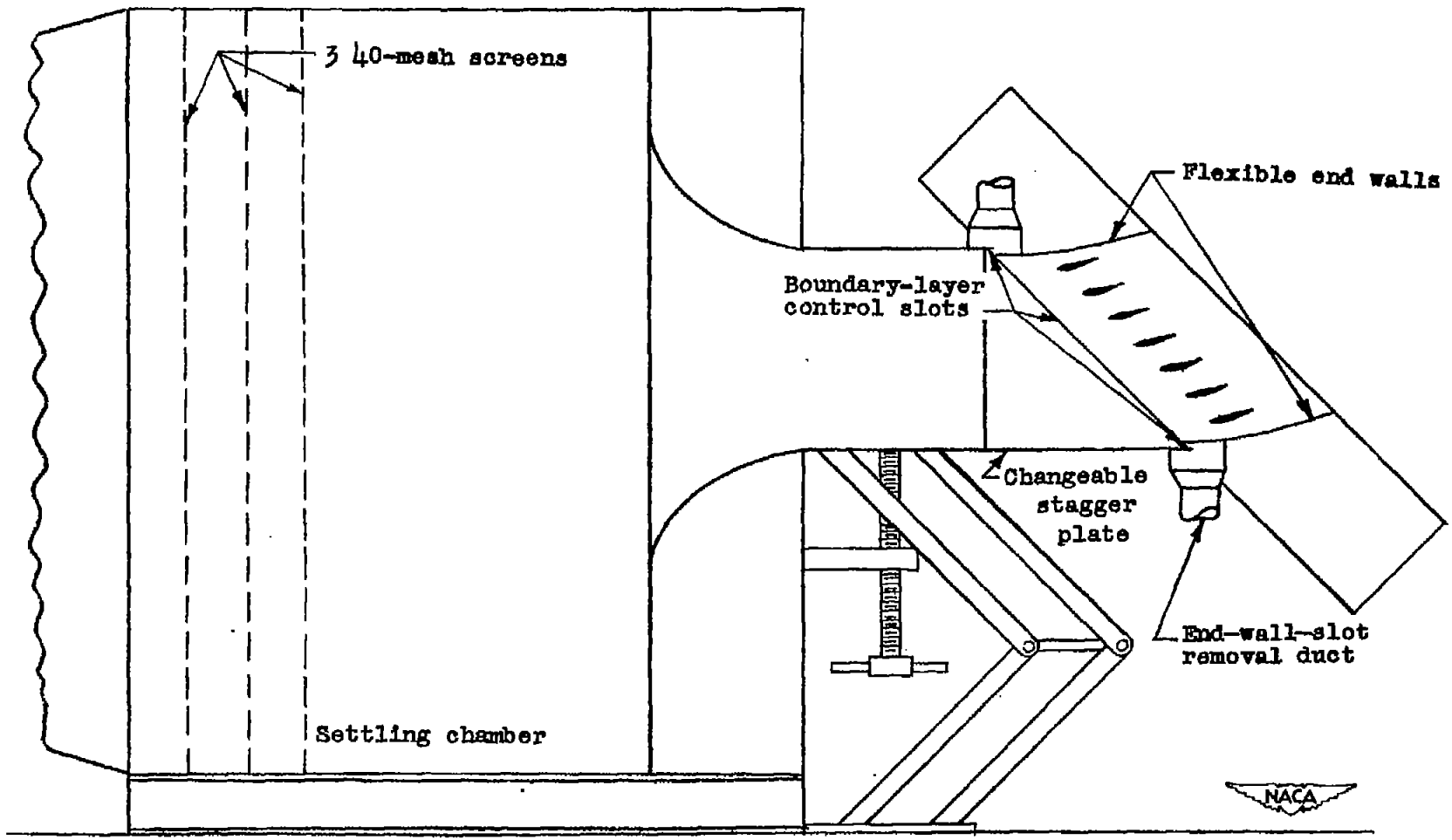

Figure 1.- Vertical cross section of two-dimensional low-speed cascade tunnels.

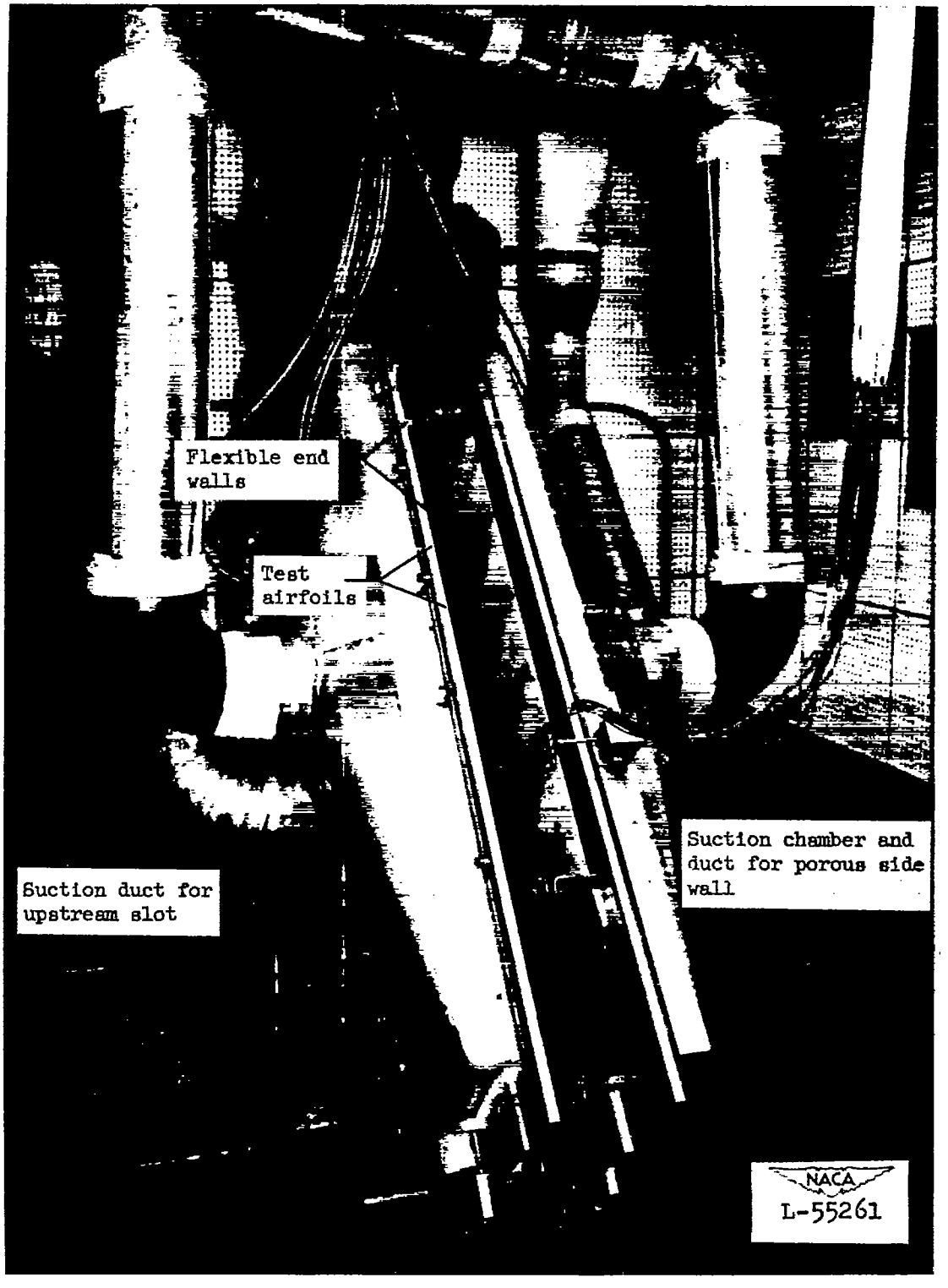

Figure 2.- Photograph of Langley 5-inch cascade tunnel equipped with porous walls.

Figure 3.- Photograph of Langley 20-inch cascade tunnel equipped with porous walls.

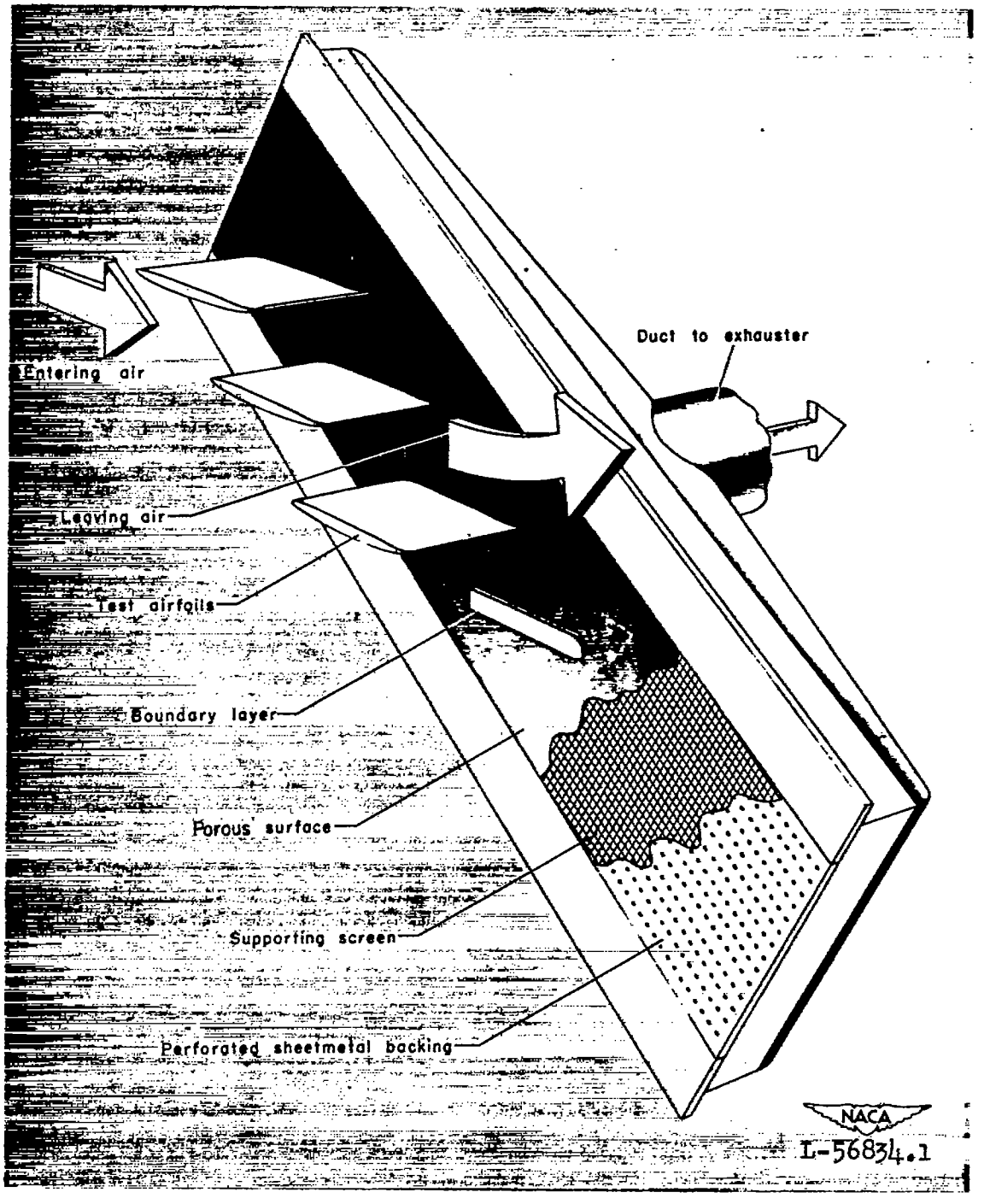

Figure 4.- Sketch showing construction of porous wall.

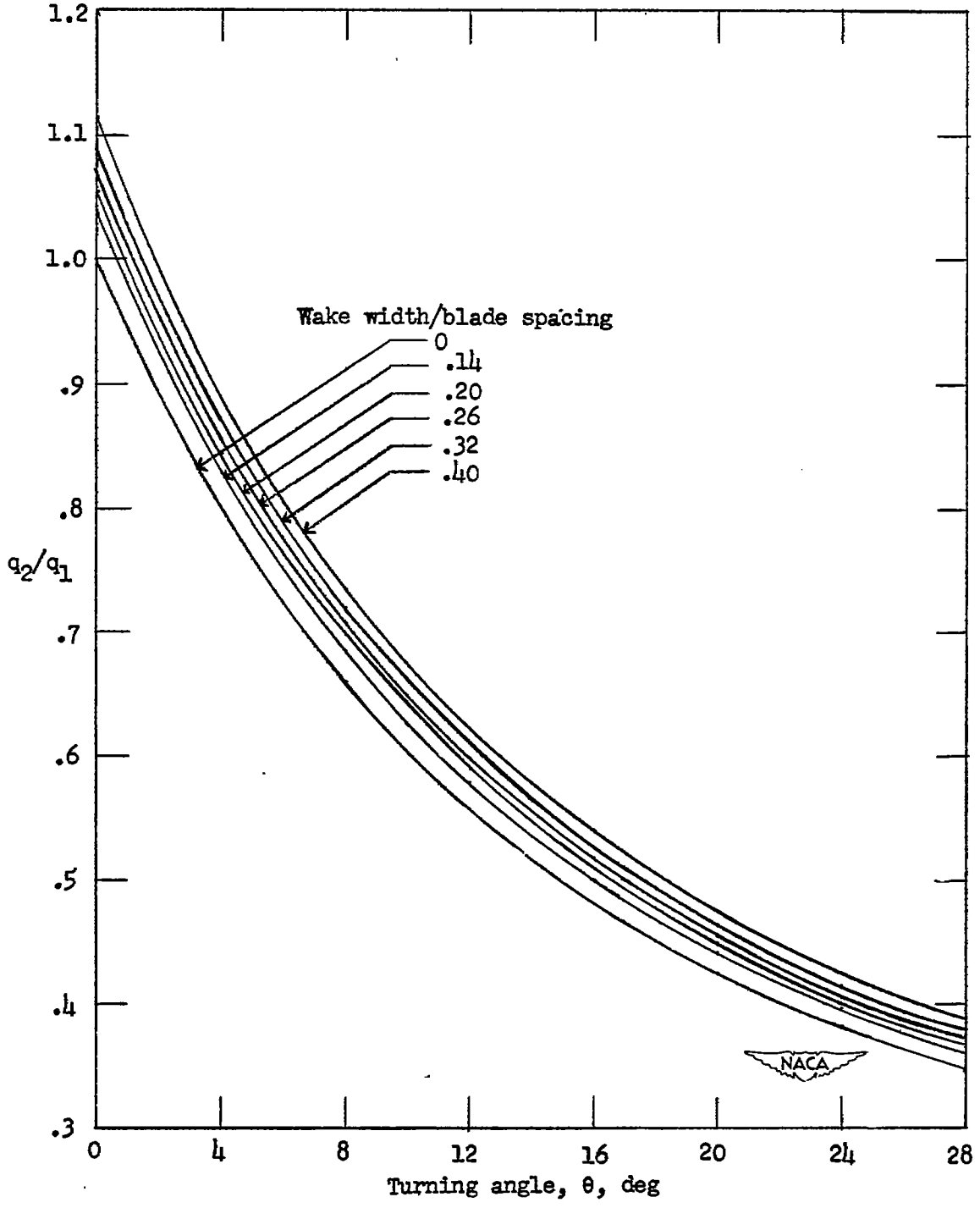

Figure 5.- Relation between dynamic-pressure ratio across cascade to turning angle. $\beta = 60^{\circ}$.

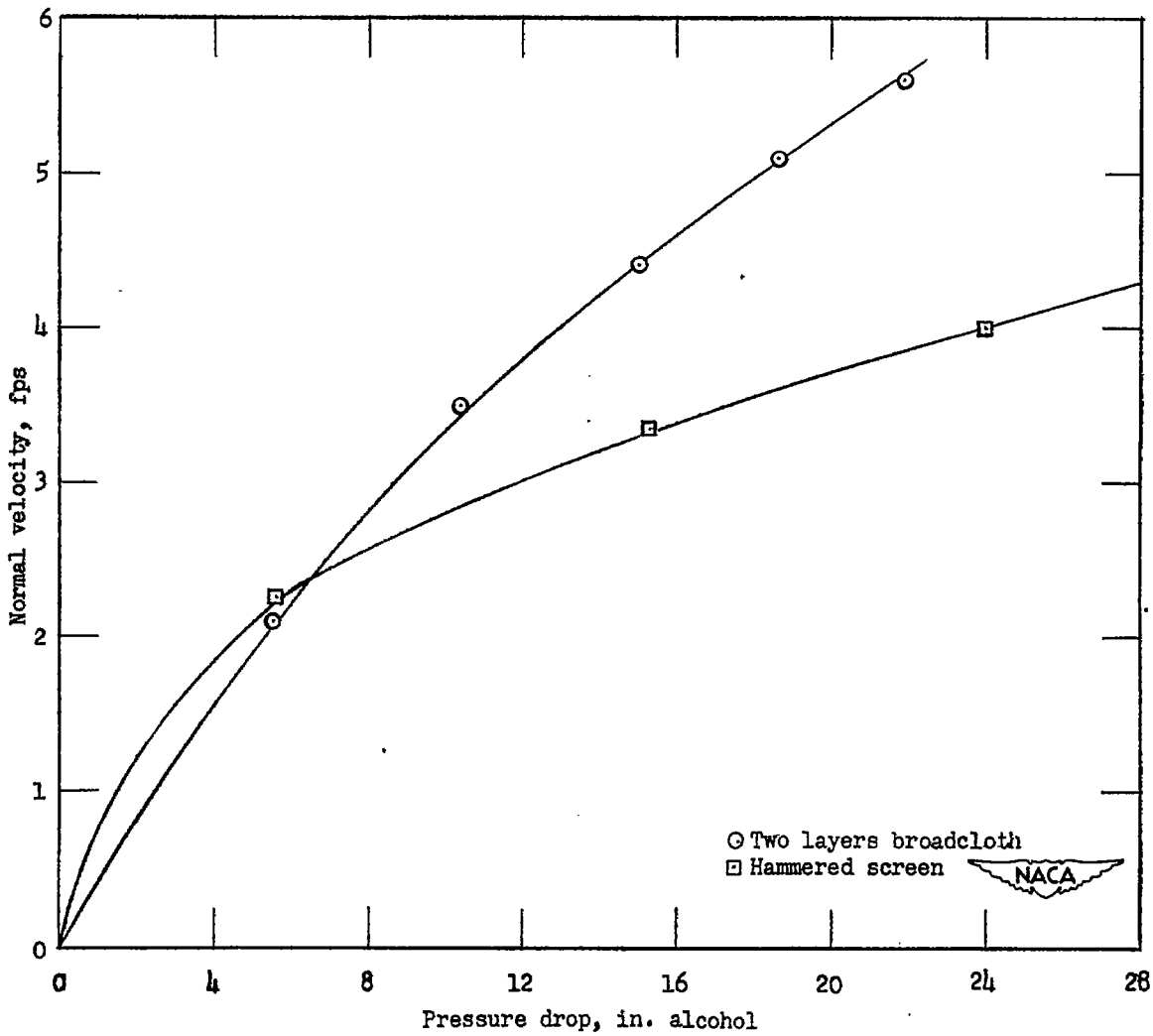

Figure 6.- Velocity through two porous materials as a function of the pressure drop.

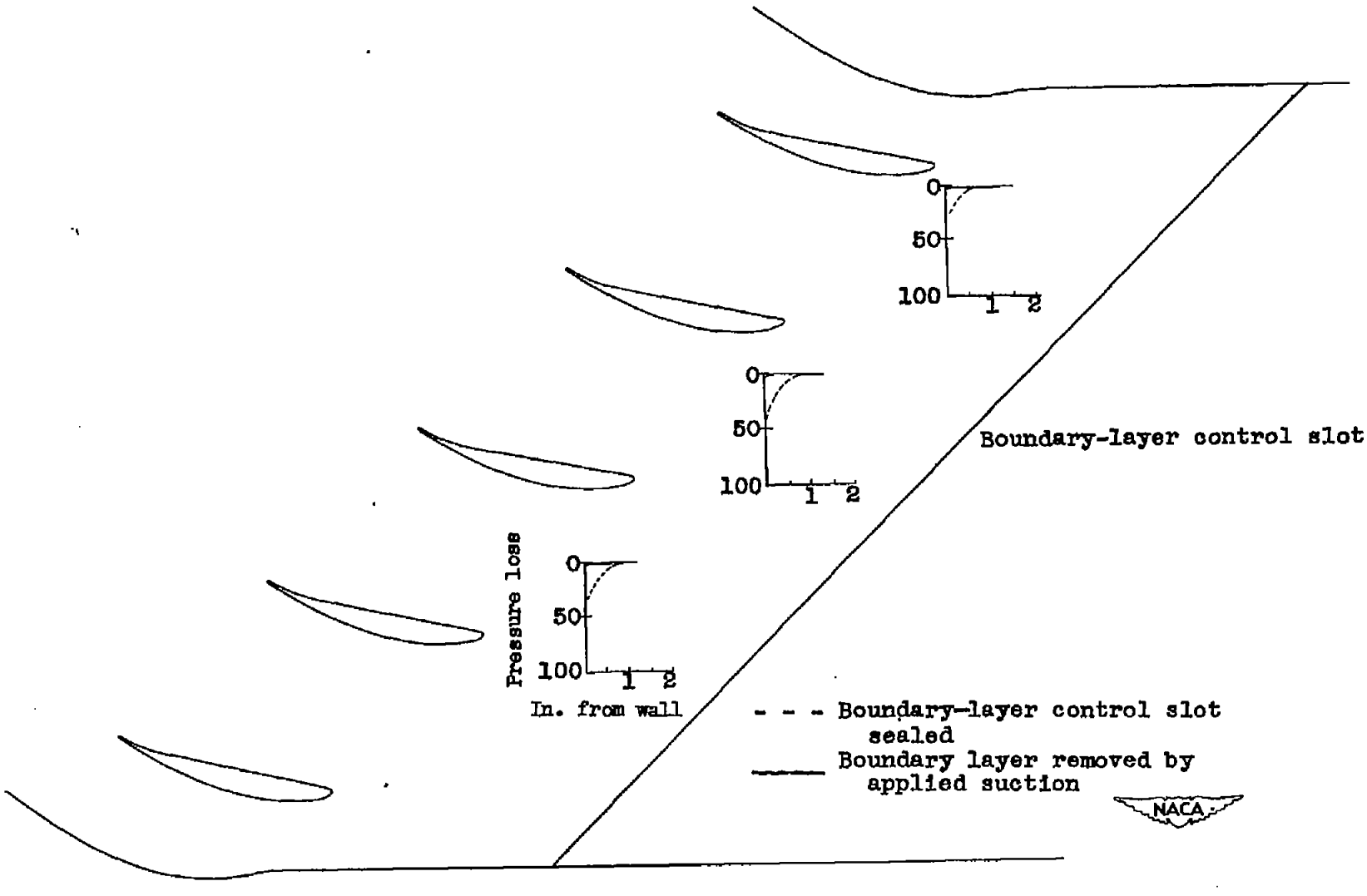

Figure 7.- Total-pressure loss in percent of entering dynamic pressure, with and without boundary-layer slot. Survey stations located at origins of small coordinate axes.

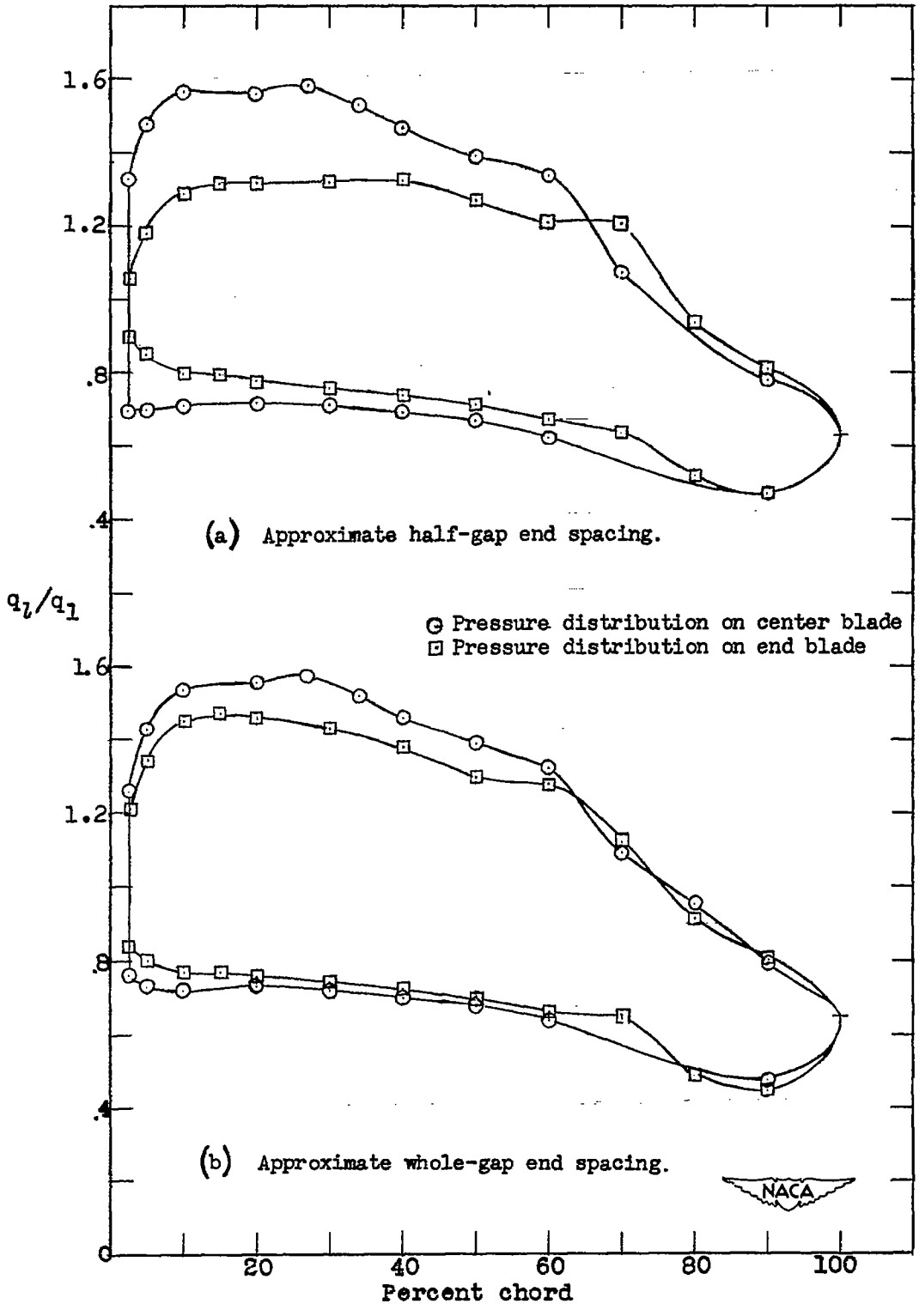

Figure 8.- Effect of end gap on the pressure distribution measured on the end blade.

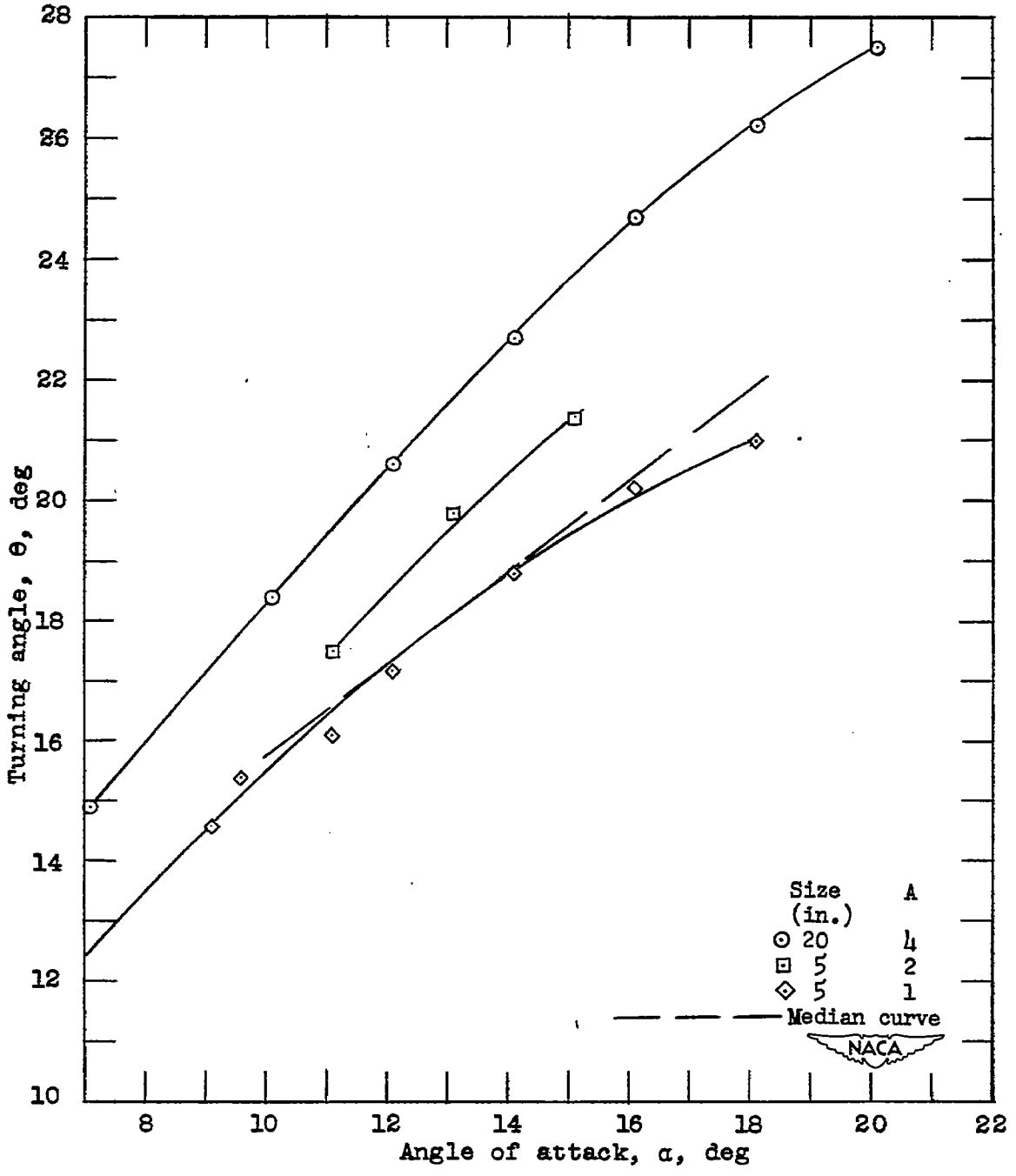

Figure 9.- Effect of aspect ratio on turning angle for solid-wall cascades. A median curve obtained from figure 10 is presented, as a dashed line, for comparison.

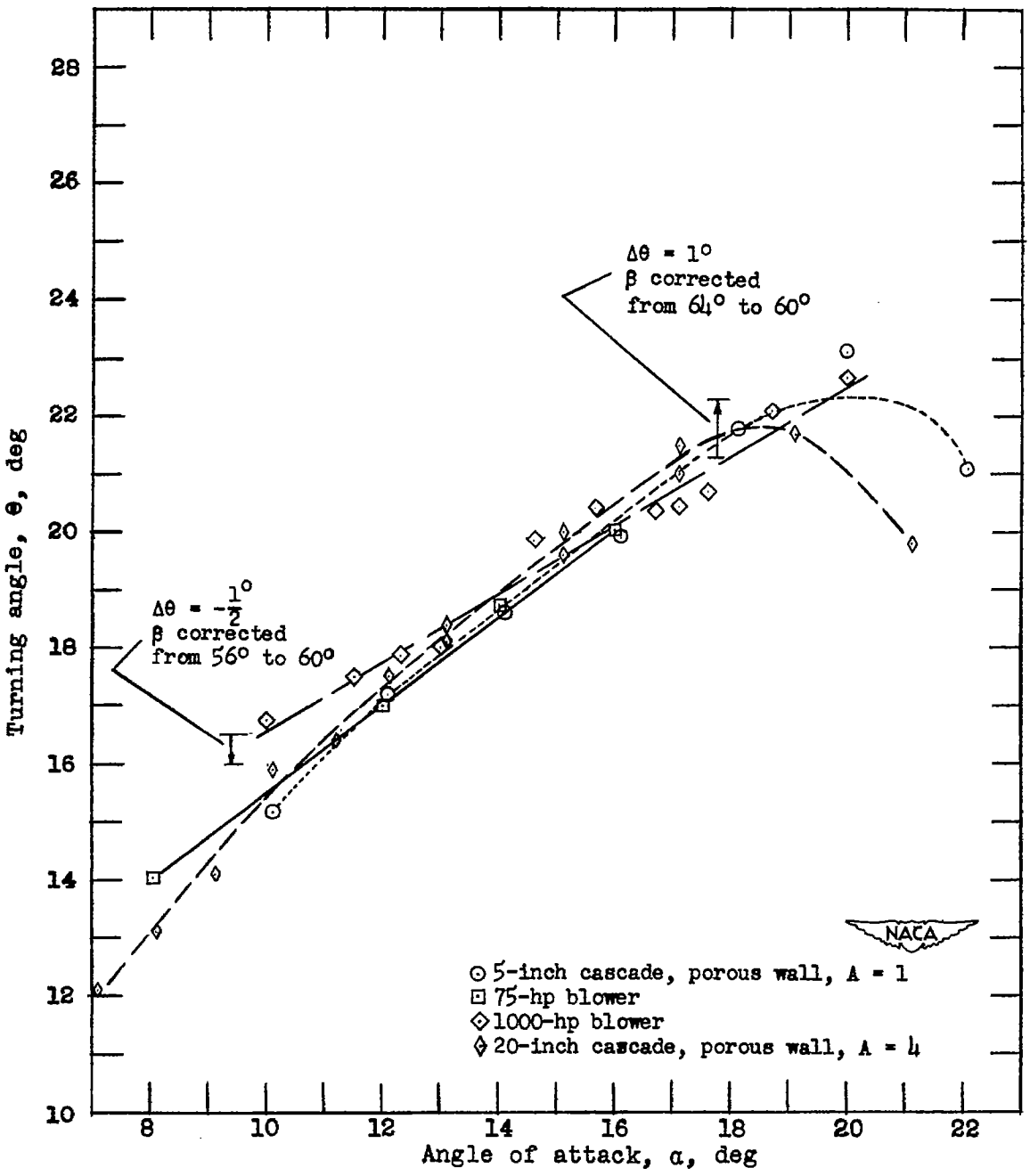

Figure 10.- Effect of aspect ratio on turning angle for porous-wall cascades. Results from two test blowers are also given. Turning-angle corrections for varying stagger angles of the 1000-horsepower blower are indicated. For 1000-horsepower blower, $\beta = 56^{\circ}$ at $\alpha = 10^{\circ}$ and $\beta = 64^{\circ}$ at $\alpha = 18^{\circ}$.

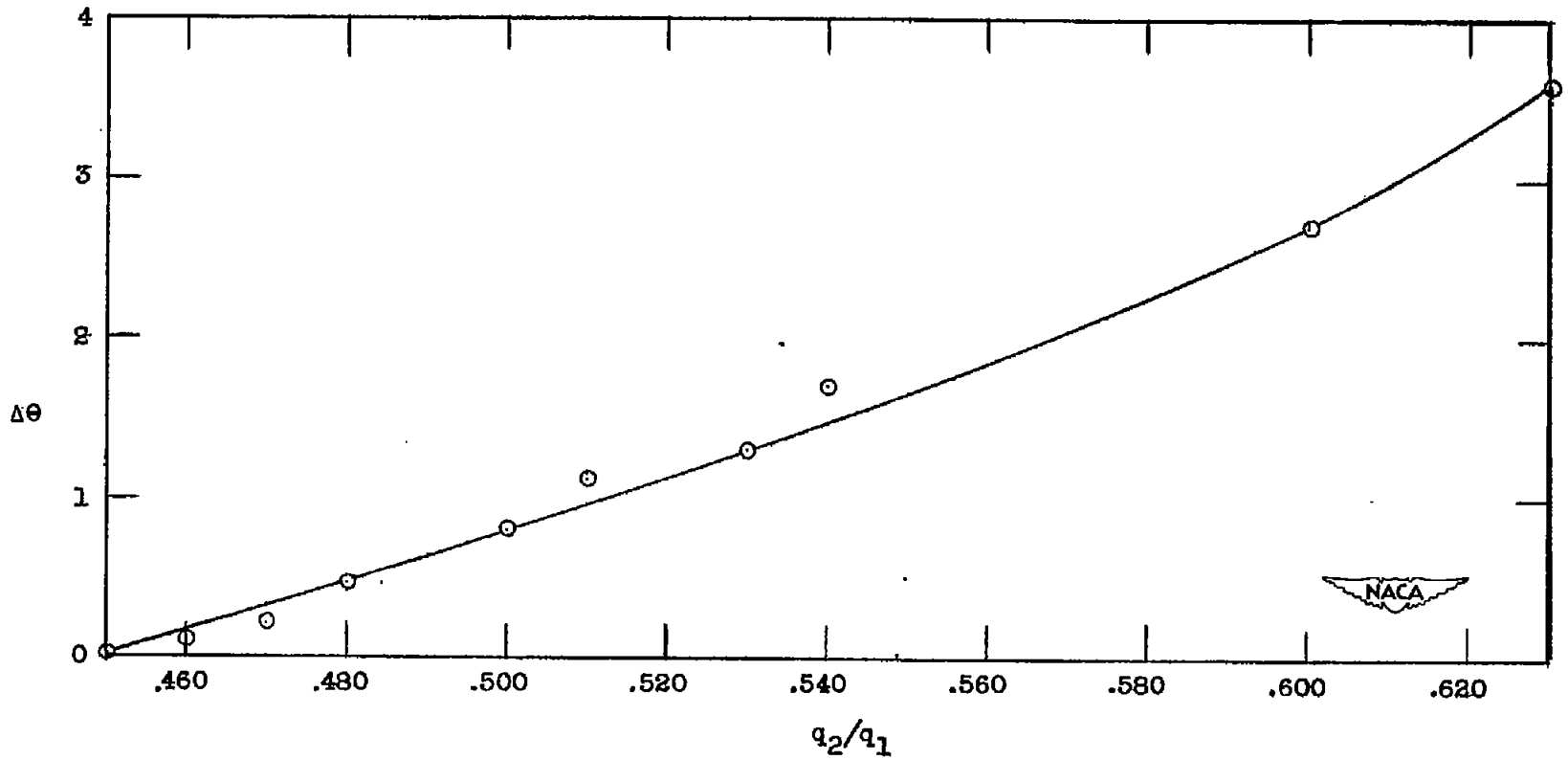

Figure 11.- Variation of turning angle with variation in pressure rise as obtained in the porous-wall cascade of aspect ratio 4. The calculated value for the measured turning angle of 20° ($\Delta\theta = 0°$) is $\frac{q_2}{q_1} = 0.450$; the value measured with no flow through the porous walls was $\frac{q_2}{q_1} = 0.630$. $\alpha = 15.1°$.

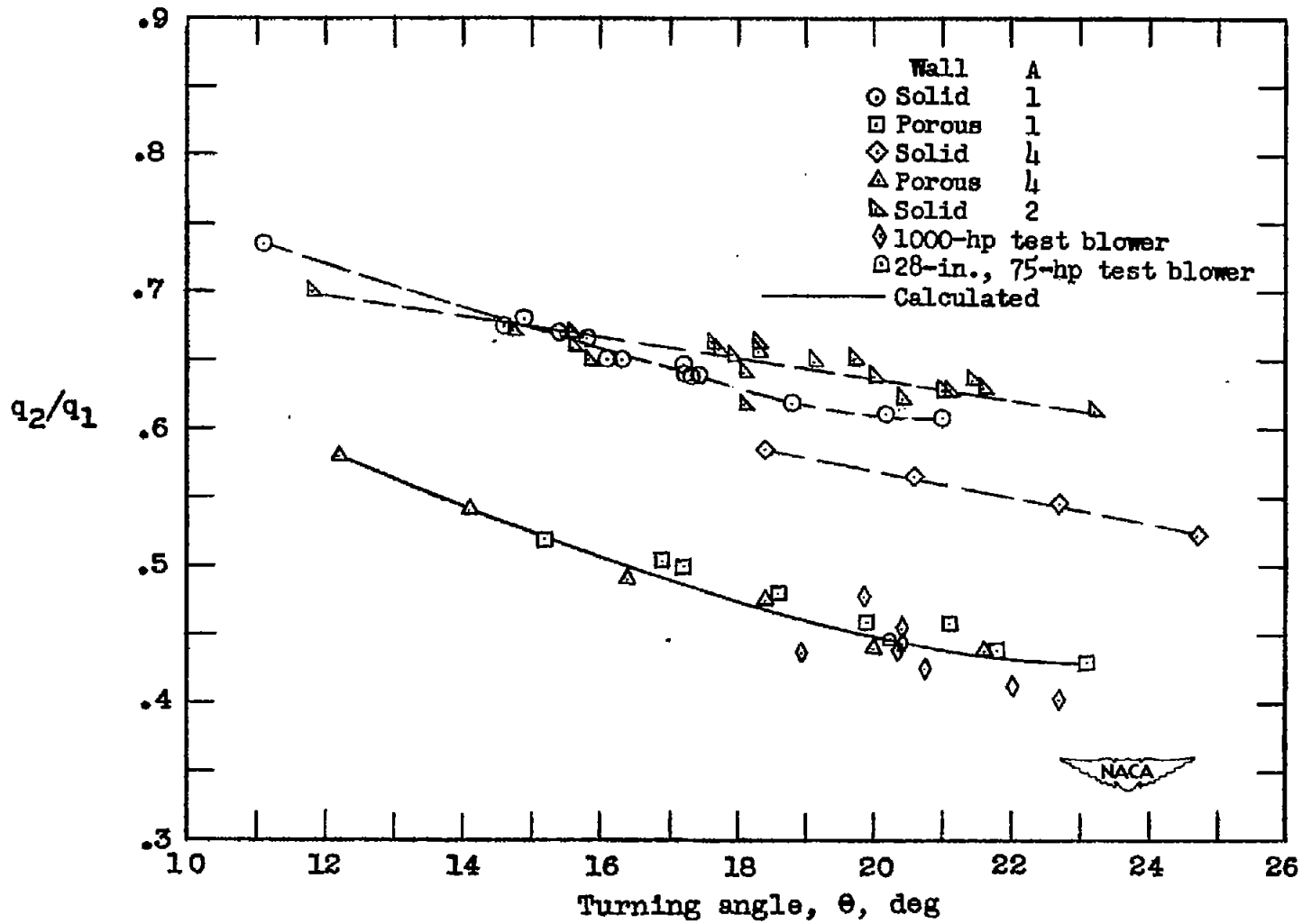

Figure 12.- Dynamic-pressure ratio as measured in the various tunnel configurations tested. The solid-line curve indicates the calculated value of q_2/q_1.

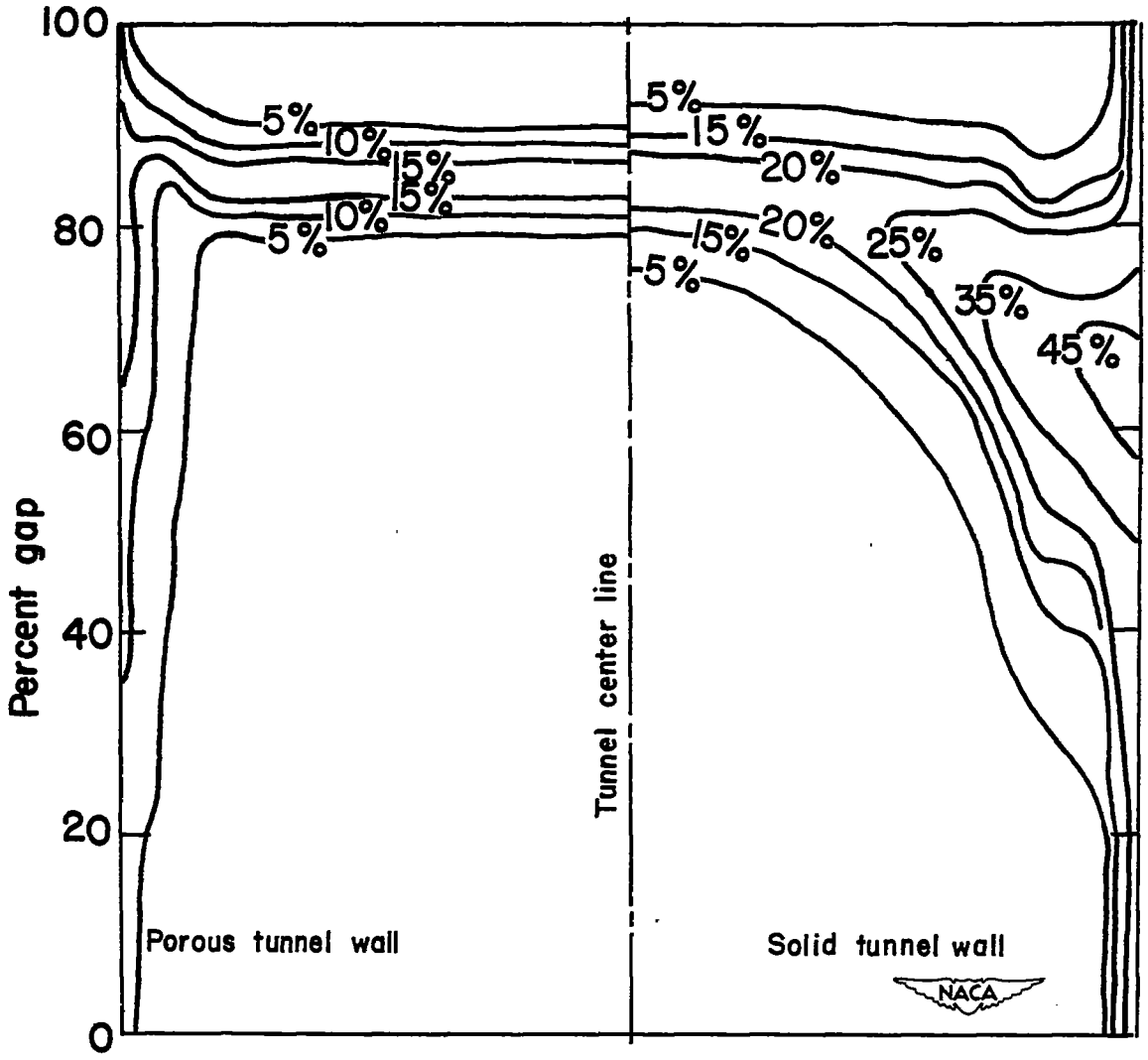

Figure 13.- Comparison of downstream total-pressure-loss contours obtained in the Langley 5-inch cascade tunnel with solid walls and with porous walls. $A = 1$; $\sigma = 1$; $\alpha = 15.1^{\circ}$.

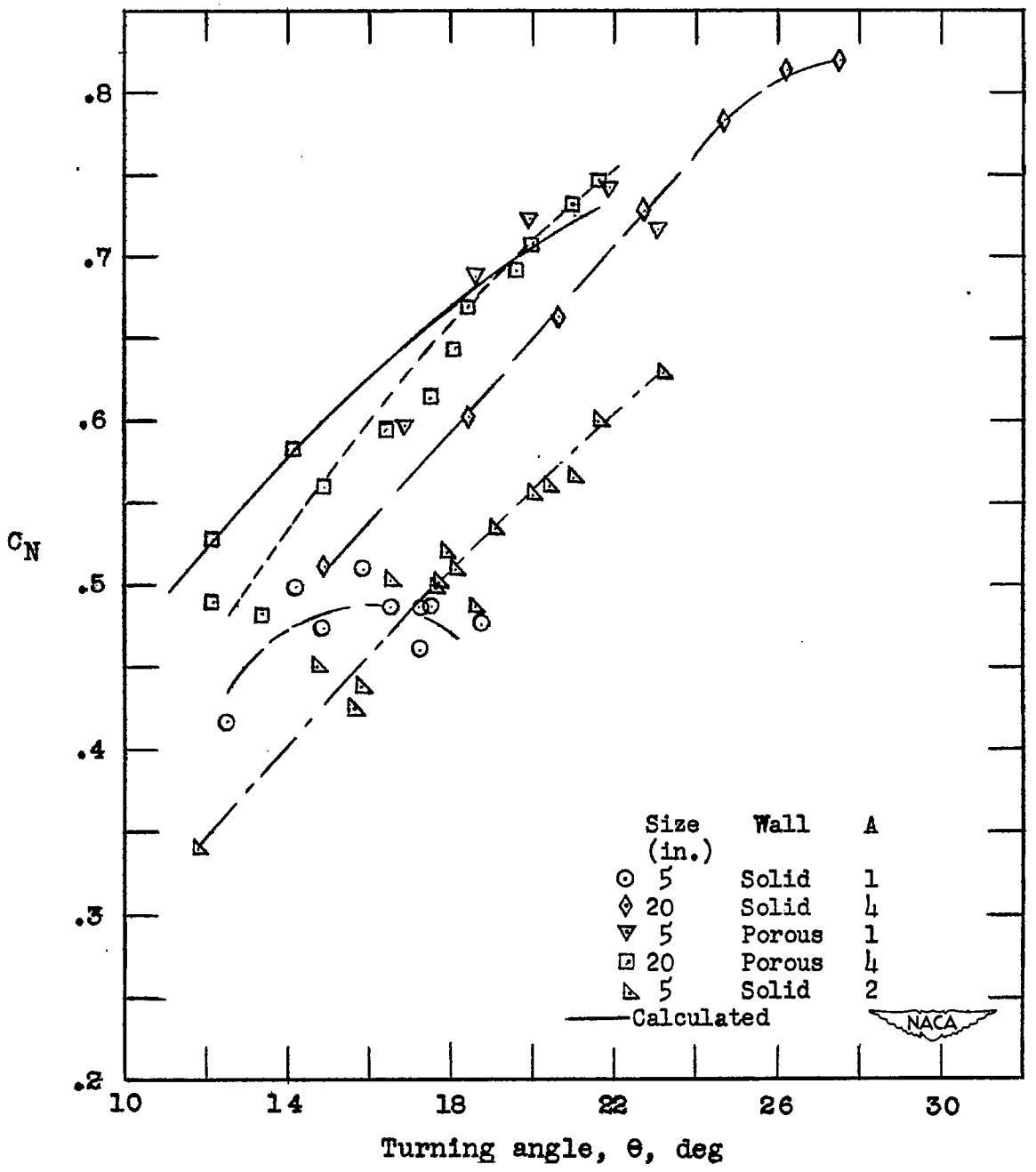

Figure 14.- Comparison of normal-force coefficient obtained in various cascades. Solid-line curve indicates calculated values of C_N.

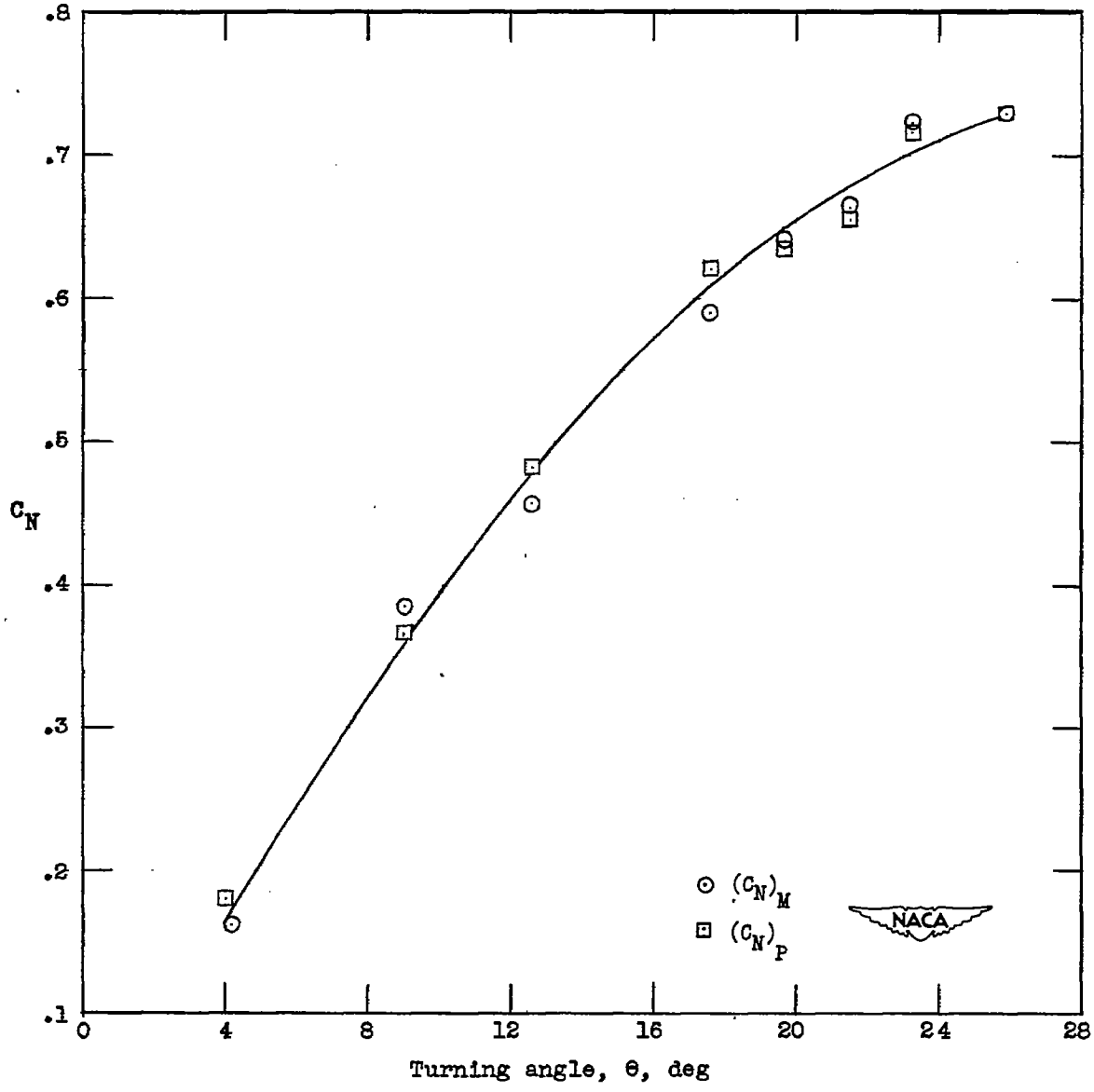

Figure 15.- Comparison of normal-force coefficient obtained by integration of blade pressure distribution and by momentum-change calculations. $\beta = 45^{\circ}$; $\sigma = 1$; porous walls.

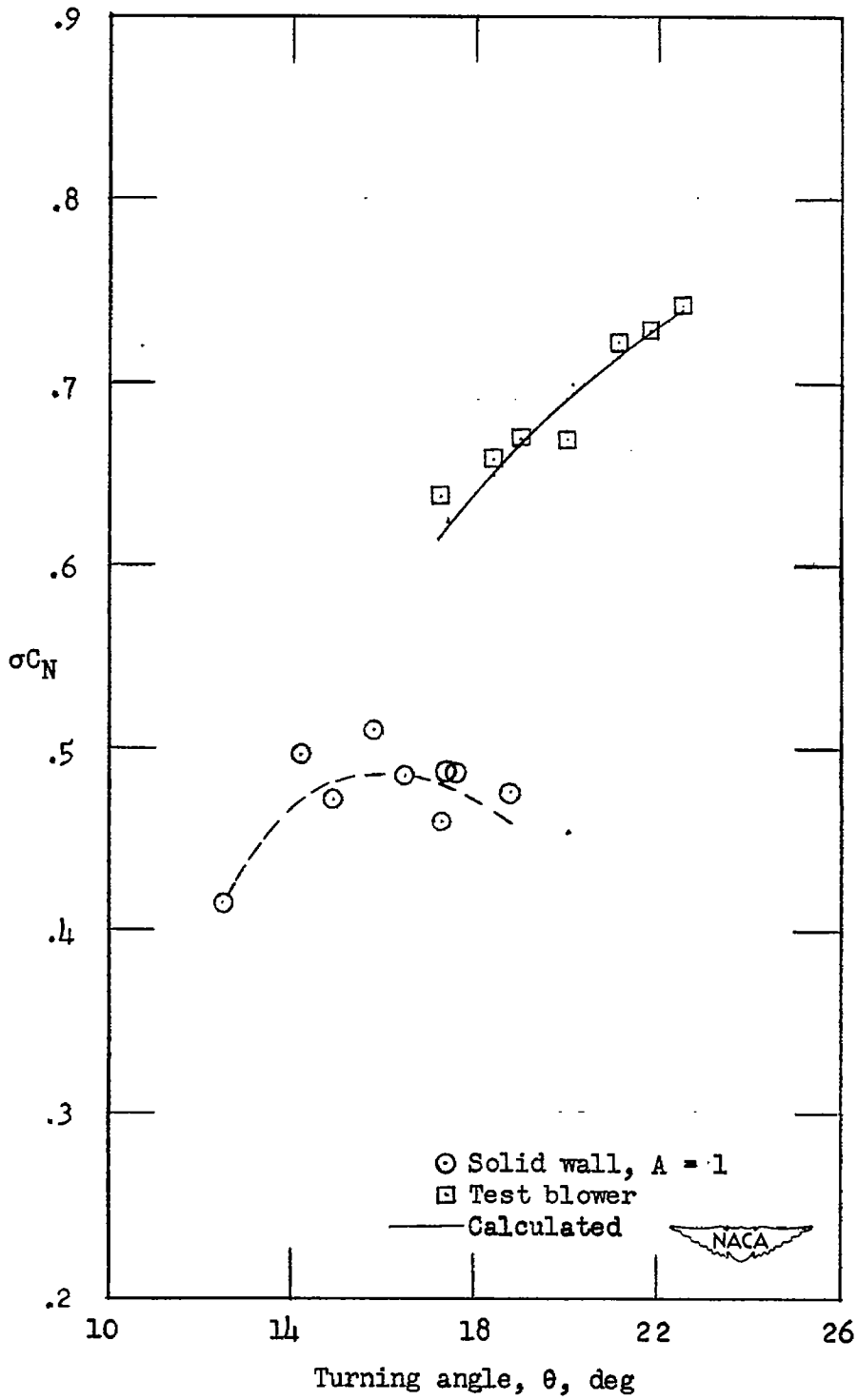

Figure 16.- Comparison of normal-force coefficient measured in the 42-inch-diameter test blower with that measured in the solid-wall cascade of A = 1. The solid curve is calculated from measured turning angle considering the appropriate stagger angle.

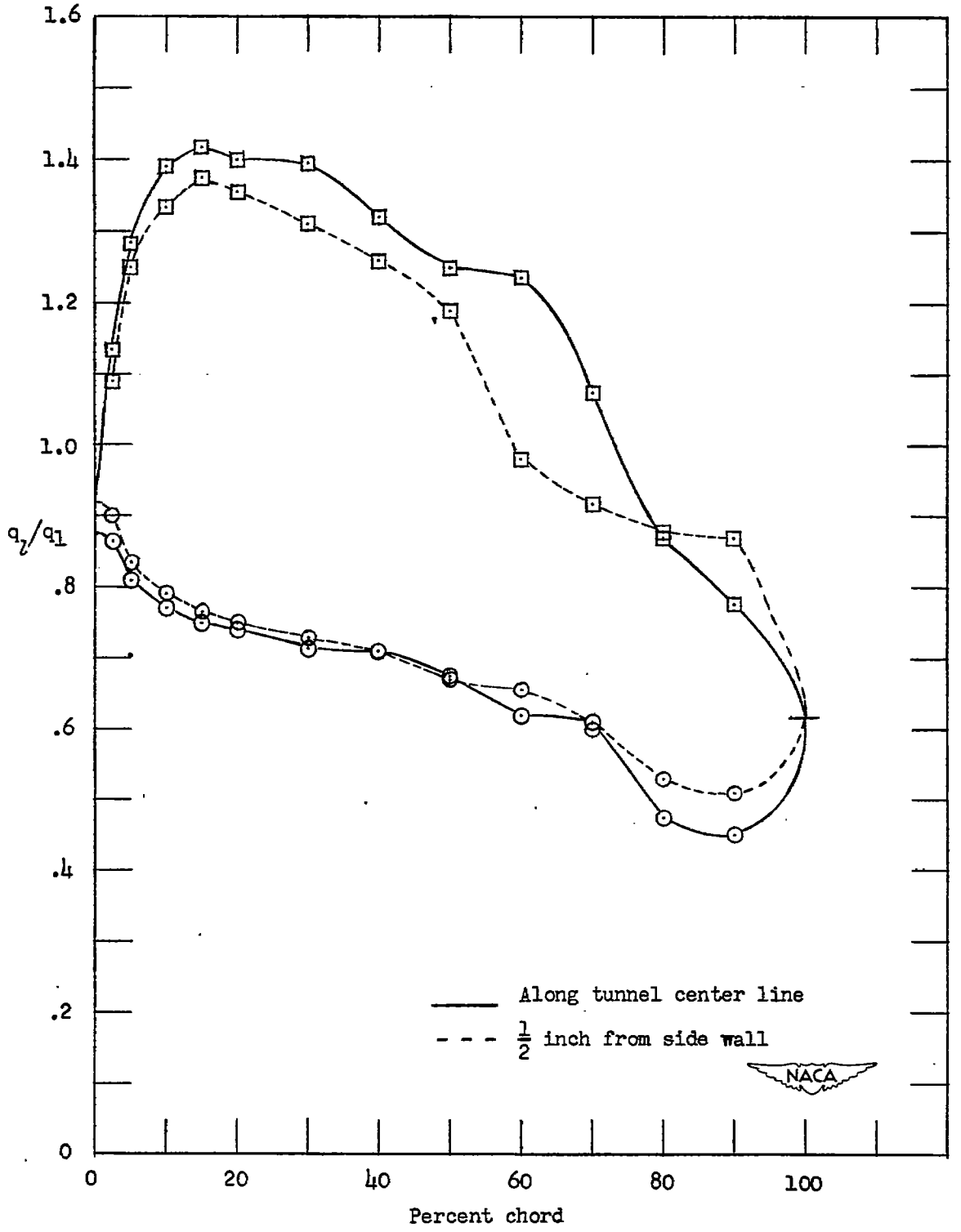

Figure 17.- Pressure distributions at two spanwise locations in the 5-inch solid-wall cascade of aspect ratio 1. $\alpha = 14.1^{\circ}$.

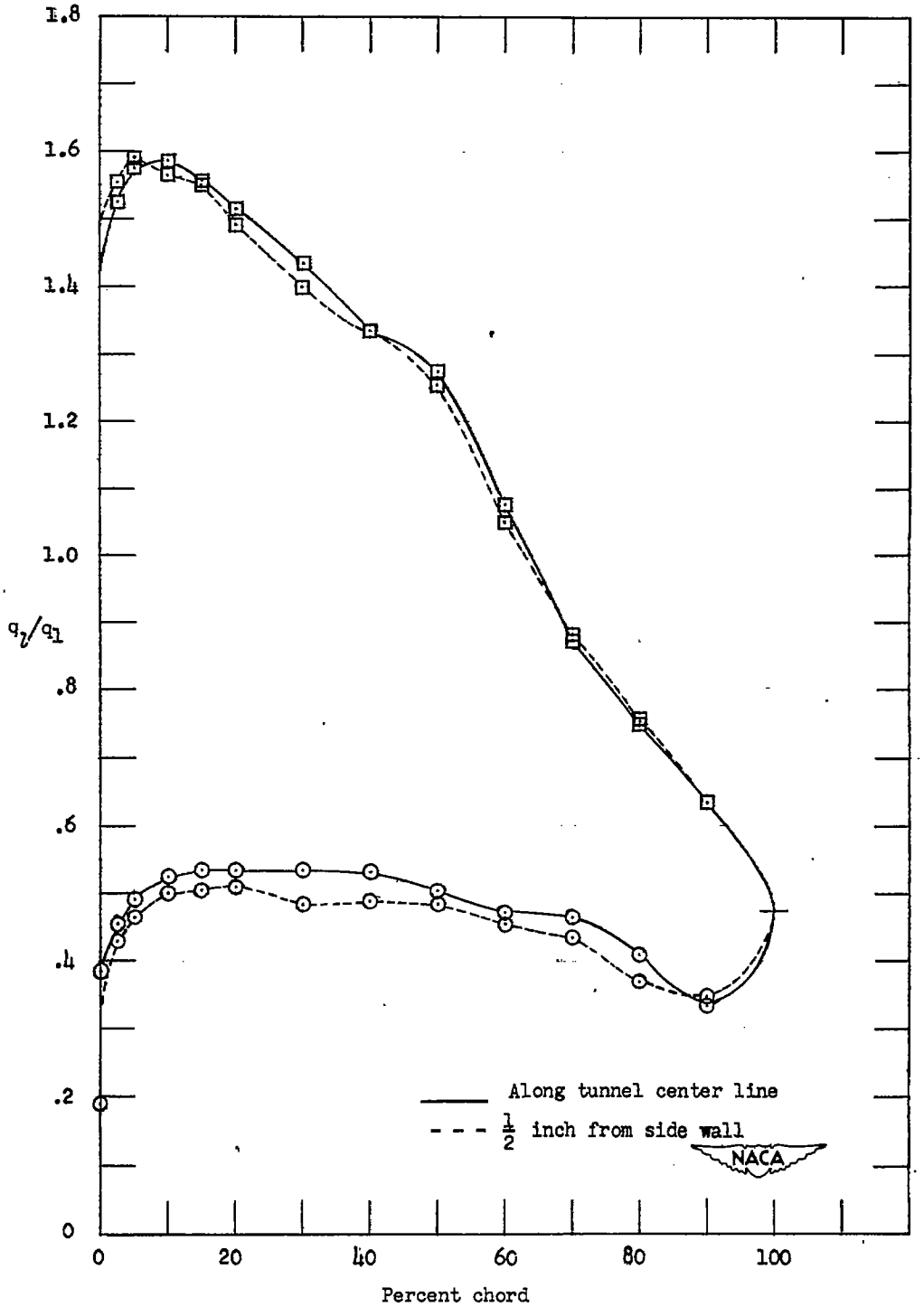

Figure 18.- Pressure distributions at two spanwise locations in the 5-inch porous-wall cascade of aspect ratio 1. $\alpha = 14.1^{\circ}$.

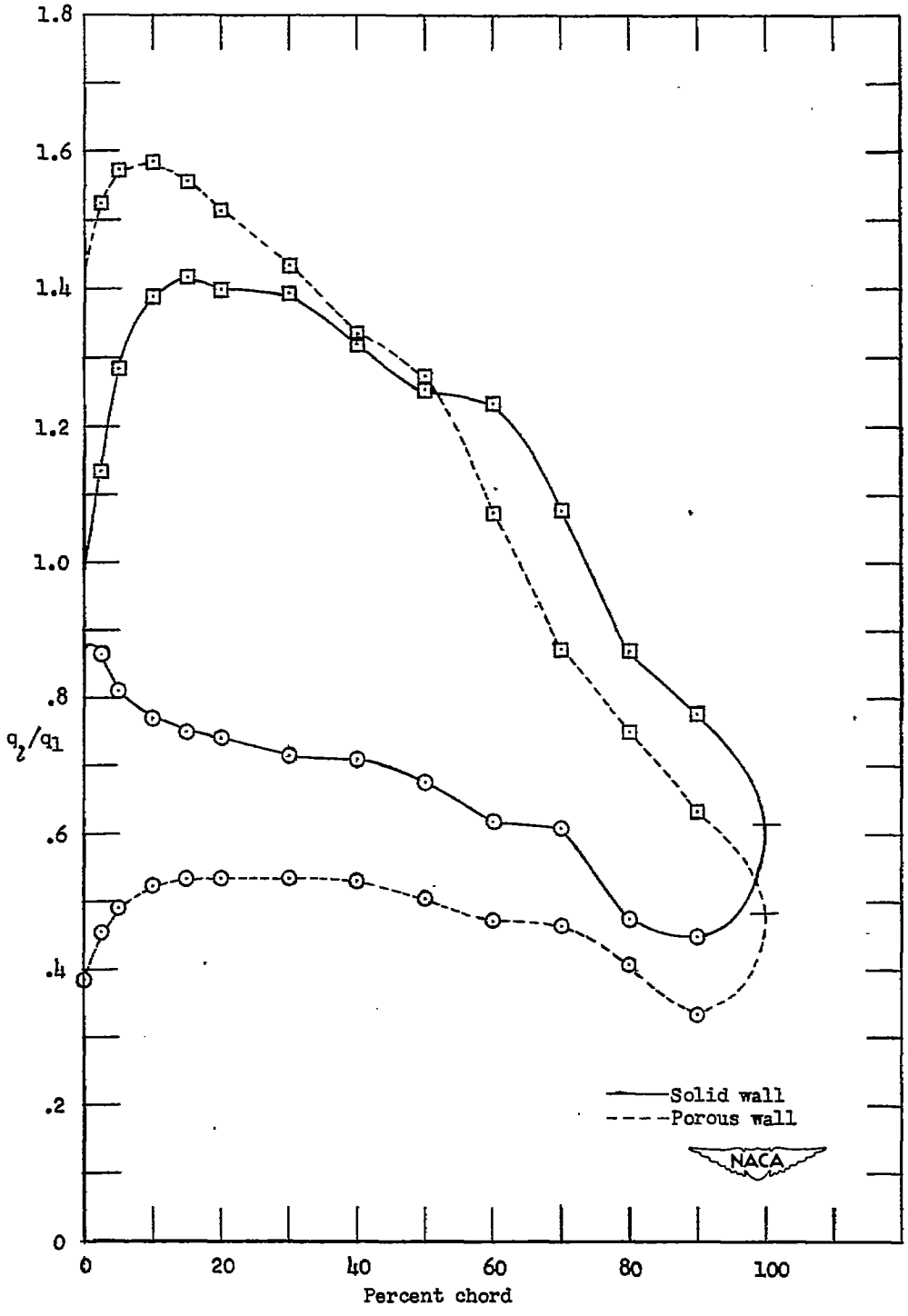

Figure 19.- Comparison of test-airfoil surface pressure distributions measured along tunnel center line with solid and with porous walls.

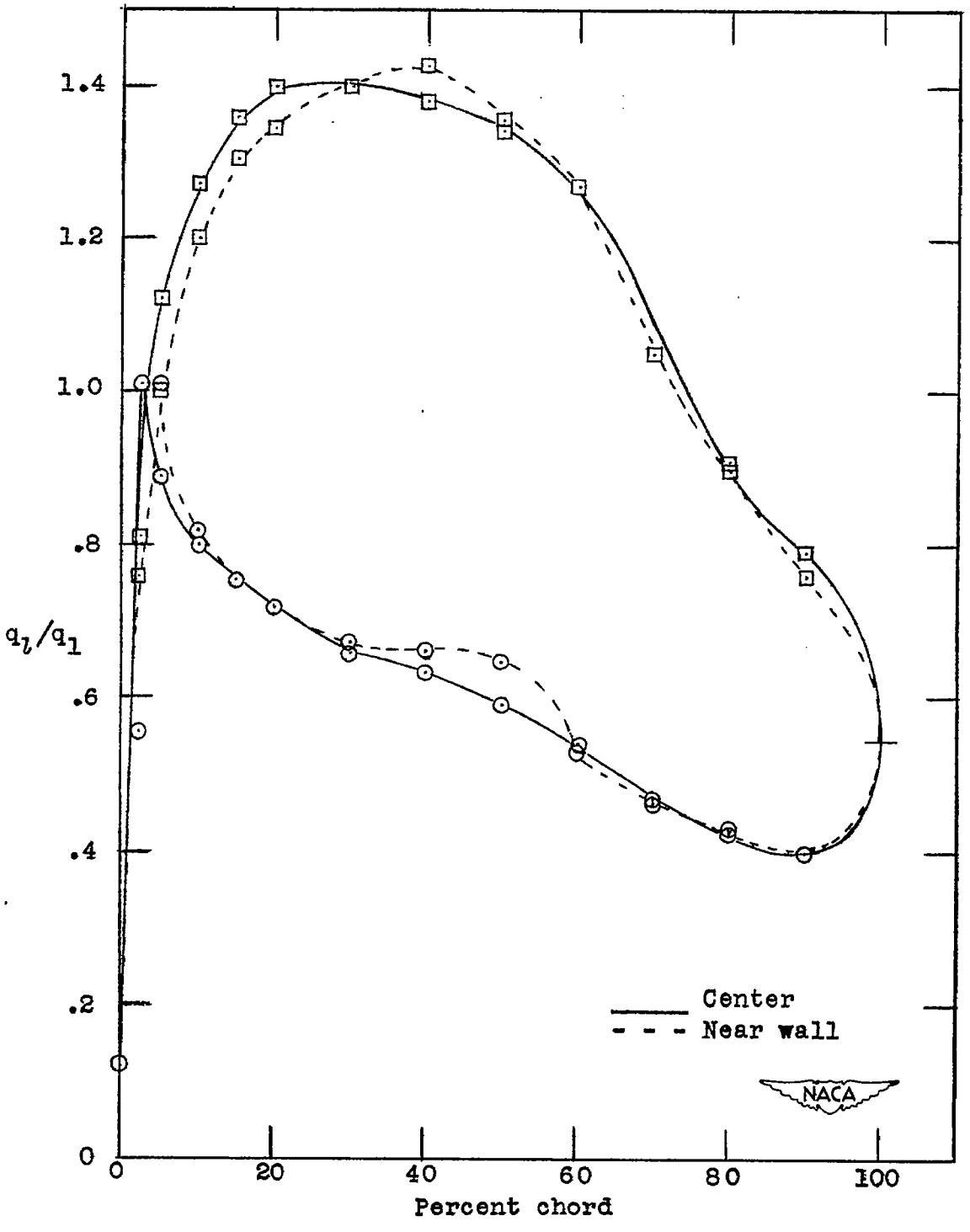

Figure 20.- Comparison of pressure distributions at two spanwise locations taken in the porous-wall cascade of aspect ratio 4, at 60° stagger, solidity of 1.

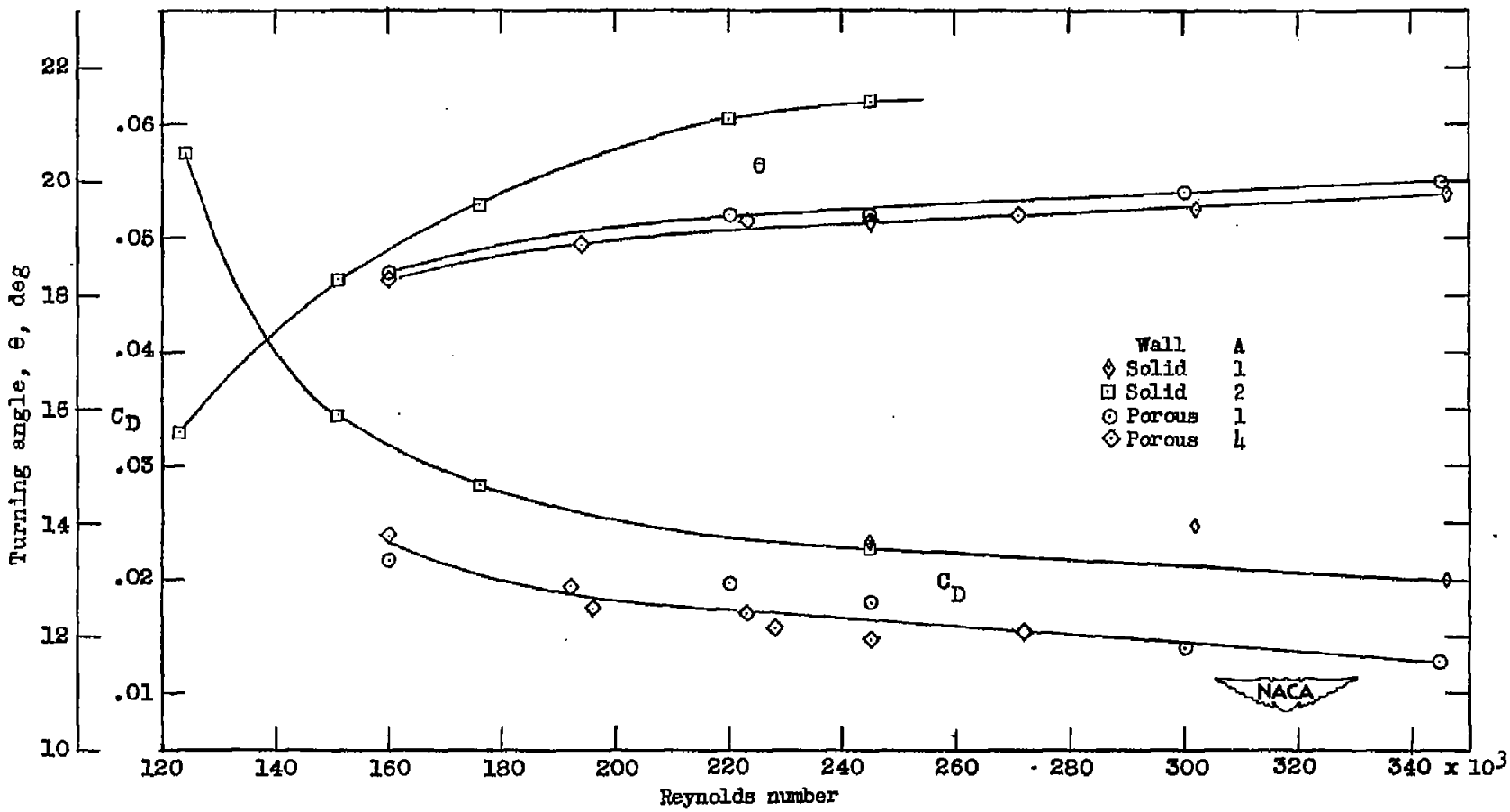

Figure 21.- Effect of Reynolds number on cascade performance. $\alpha = 15.1^{\circ}$.

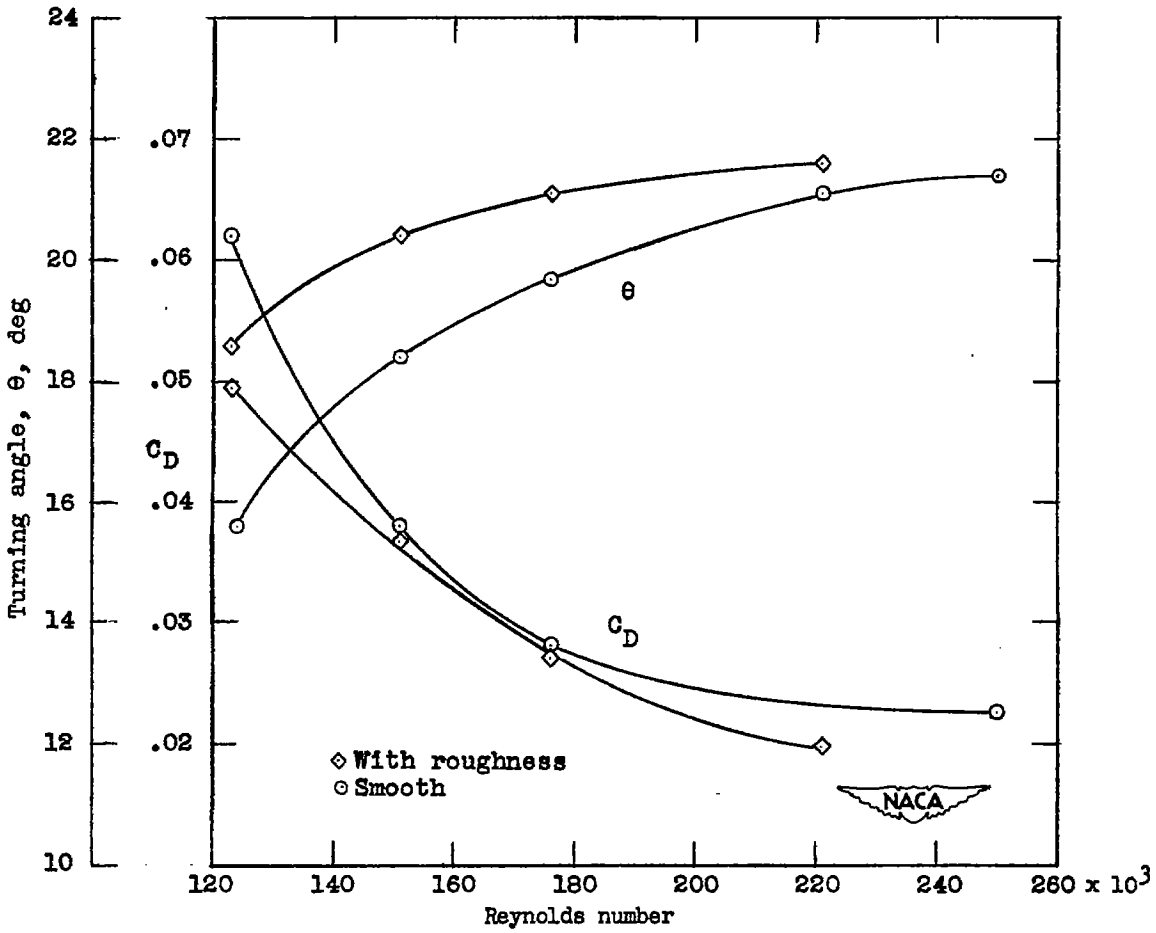

Figure 22.- Effect of roughness on cascade performance over a range of Reynolds numbers. Tests were made in 5-inch solid-wall cascade of aspect ratio 2.

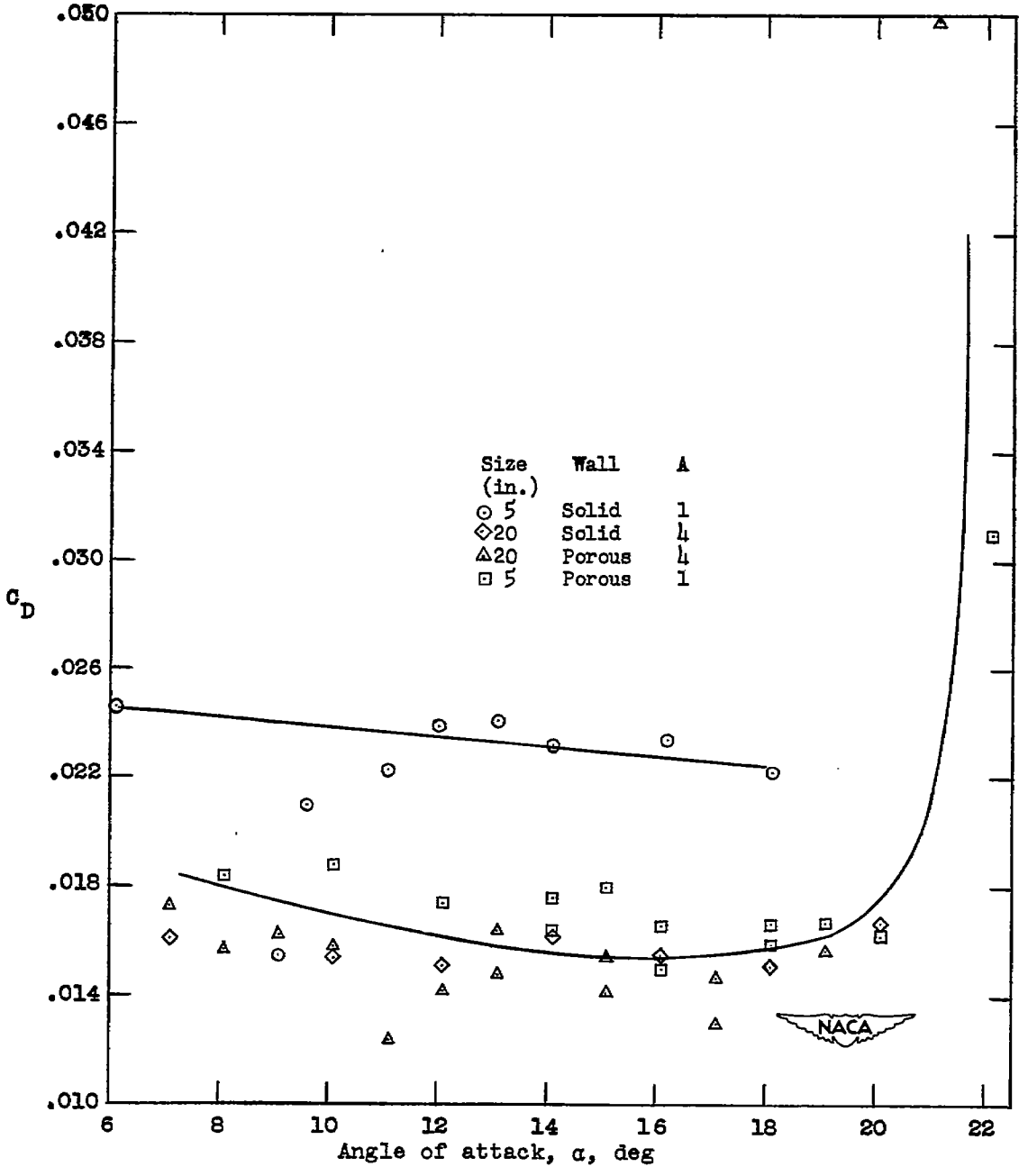

Figure 23.- Drag coefficient of the NACA 65-(12)10 airfoils at 60° stagger and solidity of 1 for various angles of attack.

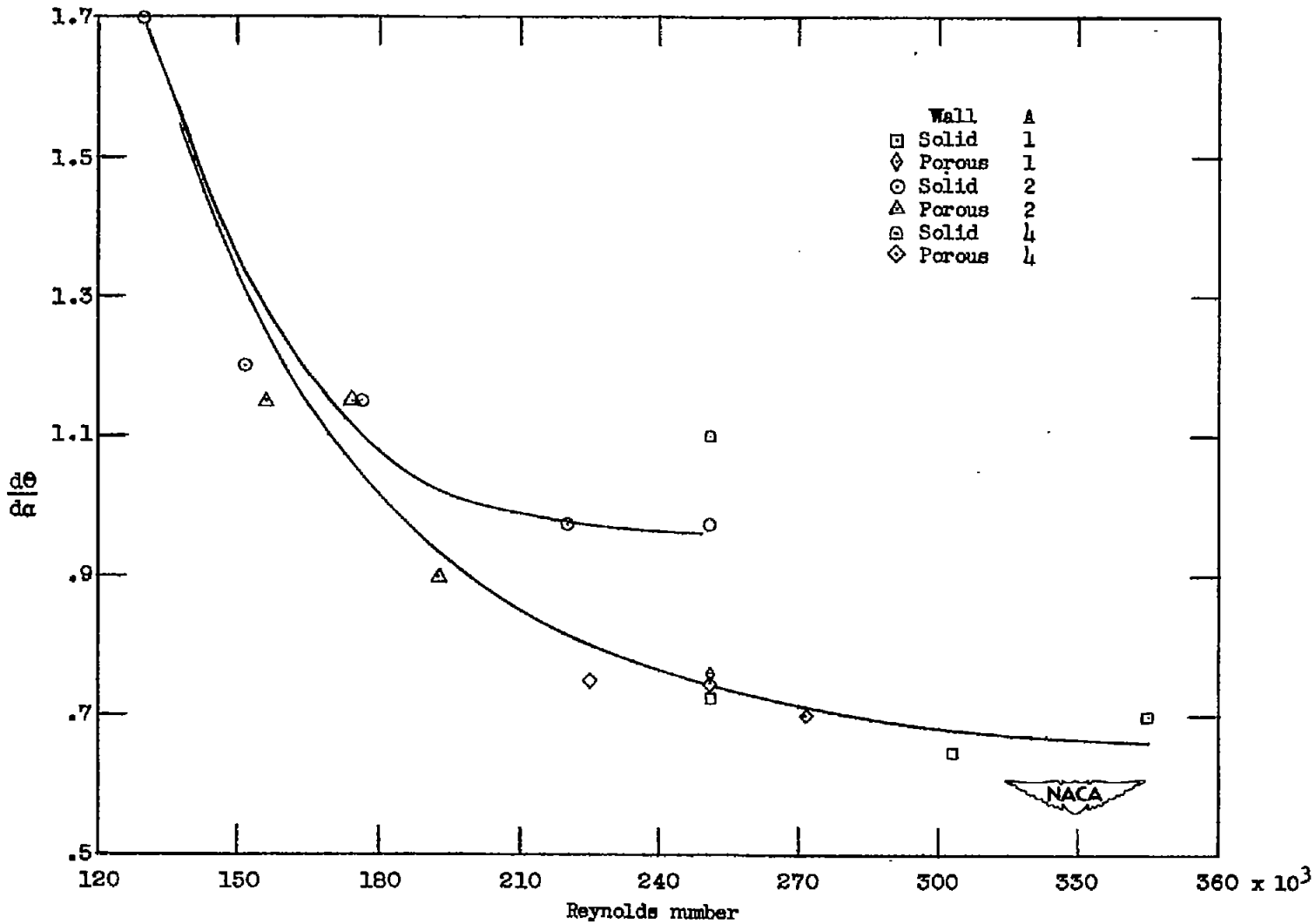

Figure 24.- Effect of Reynolds number on curve of $\frac{d\theta}{d\alpha}$.

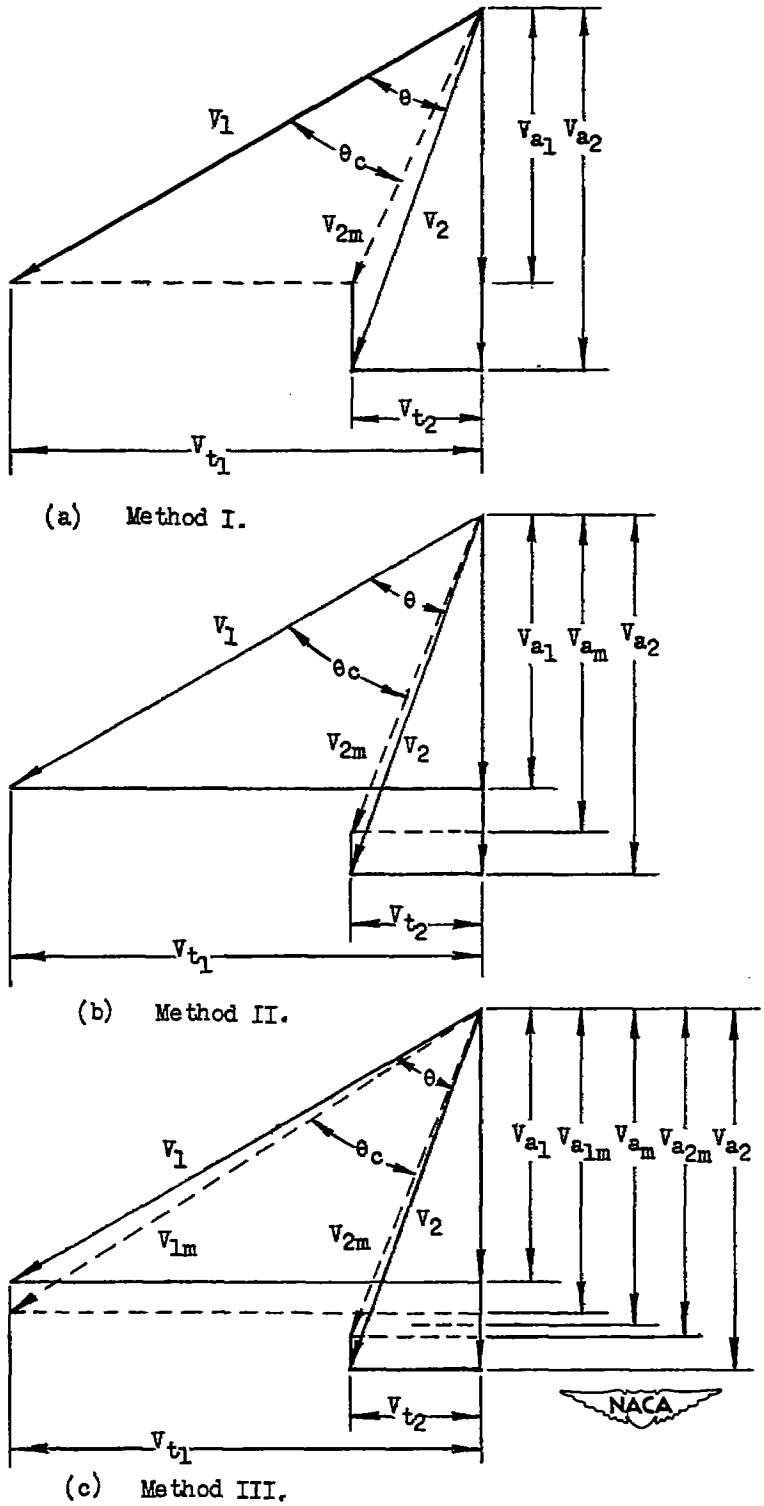

Figure 25.- Velocity diagrams illustrating several correction methods.

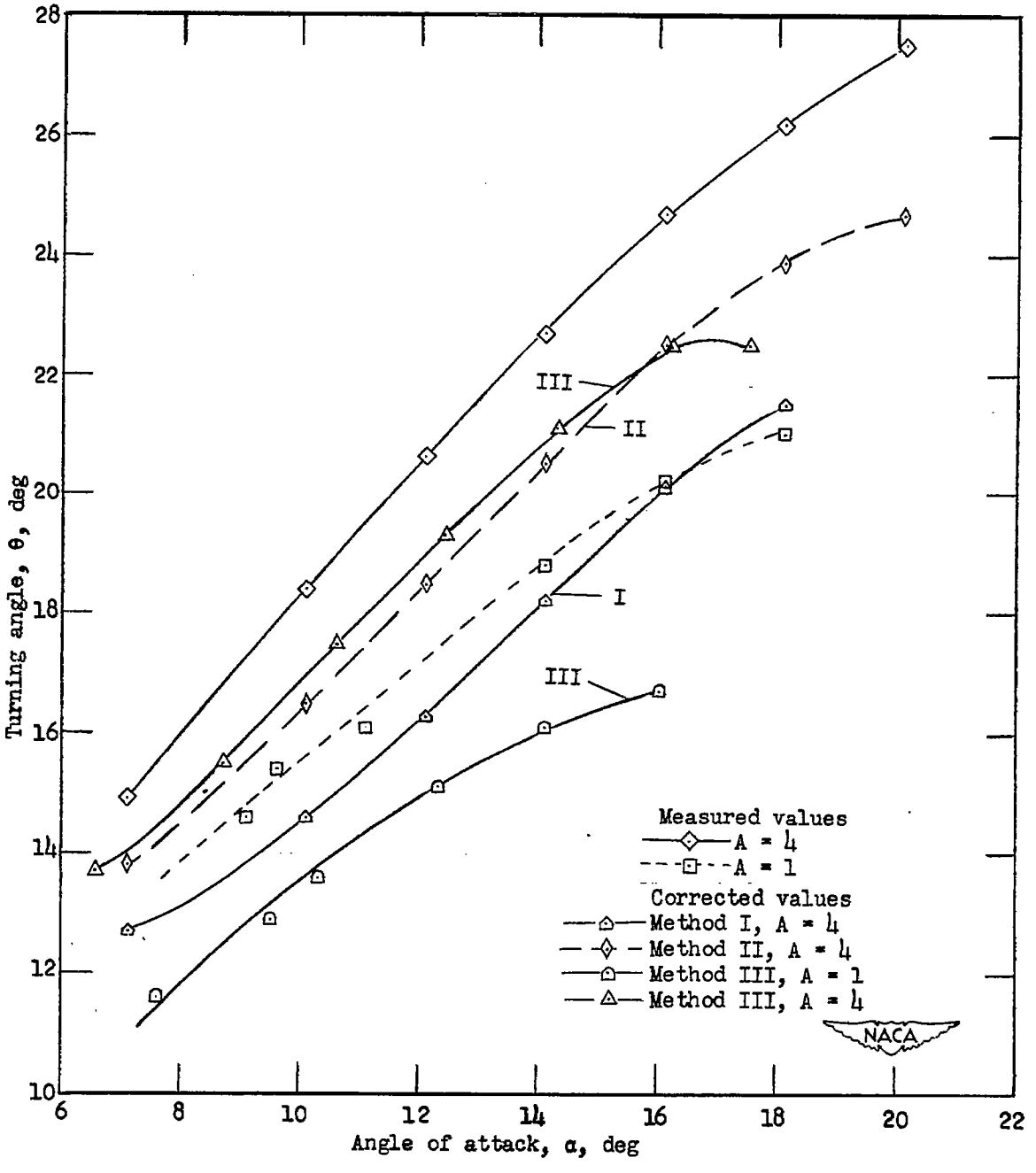

Figure 26.- Comparison of turning angles measured in the solid-wall cascades of A = 1 and A = 4 with values corrected by several methods.

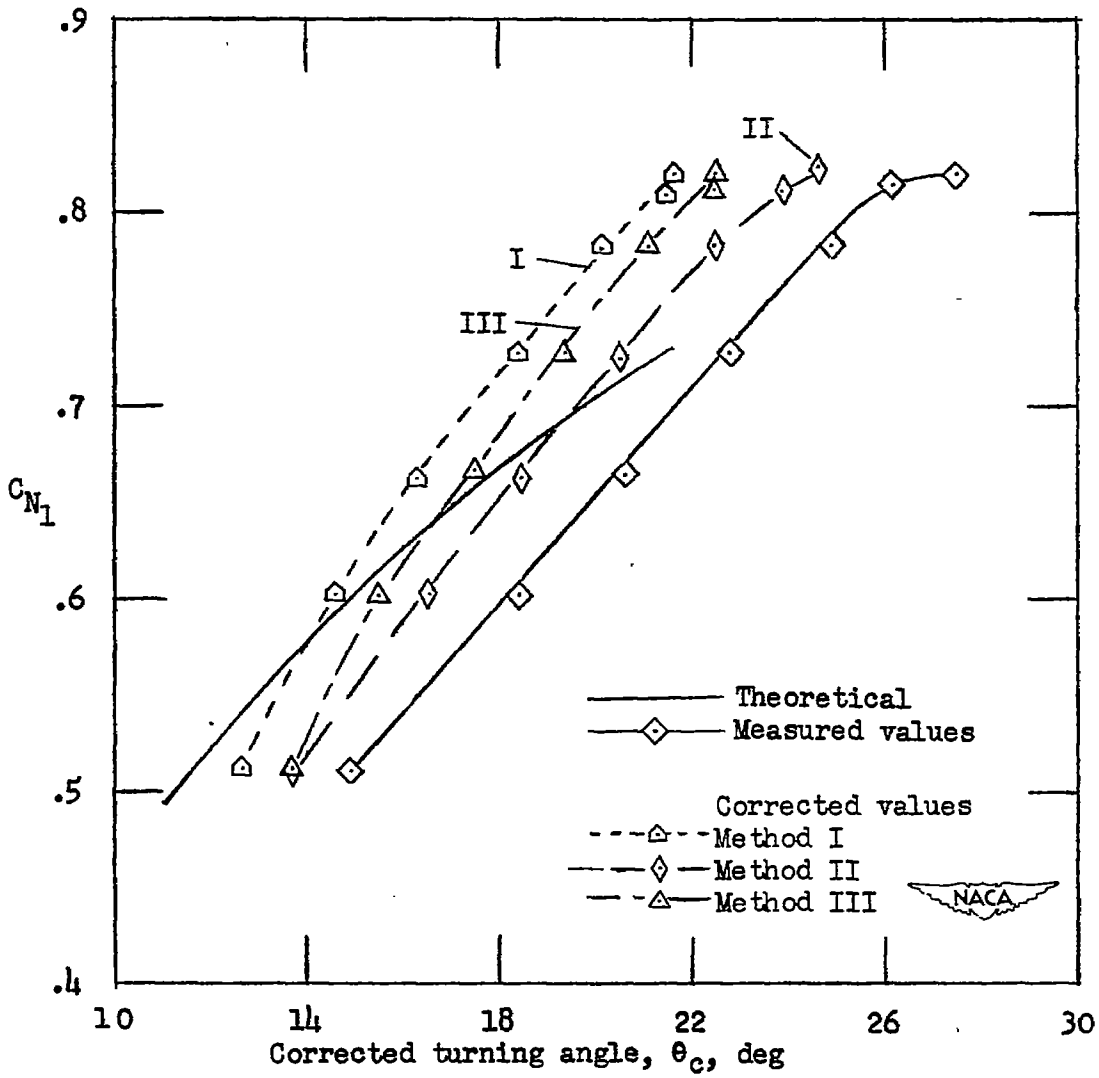

Figure 27.- Comparison of normal-force coefficients obtained in the solid-wall cascade of $A = 4$ when plotted against the measured turning angles and the turning angles corrected by three methods.

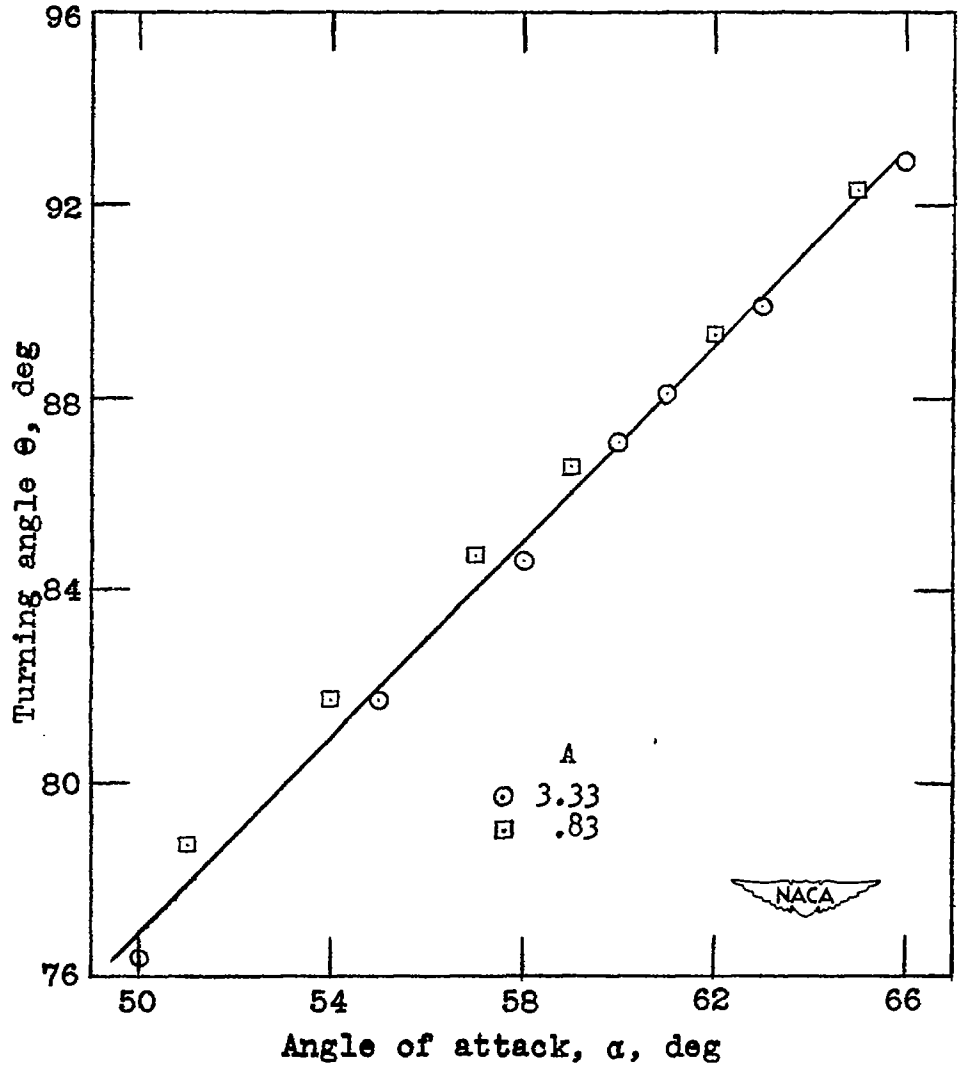

Figure 28.- Variation of turning angle with angle of attack for one turbine-blade section tested at aspect ratios of 0.83 and 3.33.

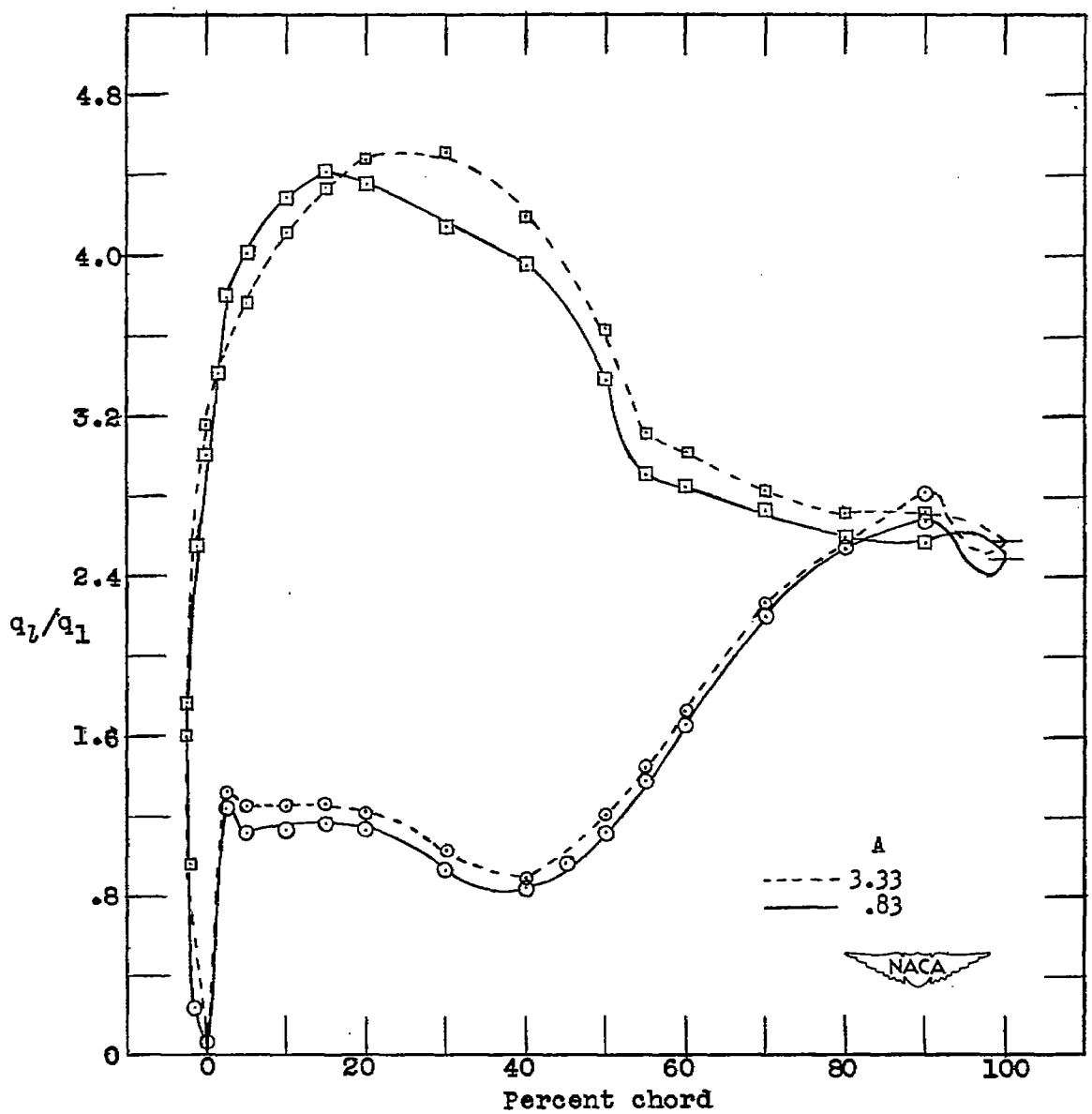

Figure 29.- Comparison of surface pressure distributions of a turbine blade of aspect ratio 0.83 and aspect ratio 3.33 in solid-wall tunnels.

NACA-Langley - 2-15-50 - 950